CORA Cork Open Research Archive
Cartlann Taighde Oscailte Chorcaí

Title	CRISPR-based gene editing enables FOXP3 gene repair in IPEX patient cells
Authors	Goodwin, M.;Lee, E.;Lakshmanan, U.;Shipp, S.;Froessl, L.;Barzaghi, F.;Passerini, L.;Narula, M.;Sheikali, A.;Lee, Ciaran M.;Bao, G.;Bauer, C. S.;Miller, H. K.;Garcia-Lloret, M.;Butte, M. J.;Bertaina, A.;Shah, A.;Pavel-Dinu, M.;Hendel, A.;Porteus, M.;Roncarolo, M. G.;Bacchetta, R.
Publication date	2020-05-06
Original Citation	Goodwin, M., Lee, E., Lakshmanan, U., Shipp, S., Froessl, L., Barzaghi, F., Passerini, L., Narula, M., Sheikali, A., Lee, C. M., Bao, G., Bauer, C. S., Miller, H. K., Garcia-Lloret, M., Butte, M. J., Bertaina, A., Shah, A., Pavel-Dinu, M., Hendel, A., Porteus, M., Roncarolo, M. G. and Bacchetta, R. (2020) 'CRISPR-based gene editing enables FOXP3 gene repair in IPEX patient cells', Science Advances, 6(19), eaaz0571 (17pp). doi: 10.1126/sciadv.aaz0571
Type of publication	Article (peer-reviewed)
Link to publisher's version	10.1126/sciadv.aaz0571
Rights	© 2020, The Authors. Some rights reserved. Exclusive licensee: American Association for the Advancement of Science. No claim to original U.S. Government Works. Distributed under a Creative Commons Attribution NonCommercial License 4.0 (CC BY-NC). - https://creativecommons.org/licenses/by-nc/4.0/
Download date	2026-11-15 12:43:51
Item downloaded from	https://hdl.handle.net/10468/10924



University College Cork, Ireland
Coláiste na hOllscoile Corcaigh

IMMUNOLOGY

CRISPR-based gene editing enables *FOXP3* gene repair in IPEX patient cells

M. Goodwin[1]*, E. Lee[1,2]*, U. Lakshmanan[1], S. Shipp[1], L. Froessl[1], F. Barzaghi[3], L. Passerini[3], M. Narula[1], A. Sheikali[1], C. M. Lee[4], G. Bao[5], C. S. Bauer[6], H. K. Miller[6], M. Garcia-Lloret[7], M. J. Butte[7], A. Bertaina[1], A. Shah[1], M. Pavel-Dinu[1], A. Hendel[1,8], M. Porteus[1,2], M. G. Roncarolo[1,2], R. Bacchetta[1†]

Copyright © 2020 The Authors, some rights reserved; exclusive licensee American Association for the Advancement of Science. No claim to original U.S. Government Works. Distributed under a Creative Commons Attribution NonCommercial License 4.0 (CC BY-NC).

The prototypical genetic autoimmune disease is immune dysregulation polyendocrinopathy enteropathy X-linked (IPEX) syndrome, a severe pediatric disease with limited treatment options. IPEX syndrome is caused by mutations in the forkhead box protein 3 (*FOXP3*) gene, which plays a critical role in immune regulation. As a monogenic disease, IPEX is an ideal candidate for a therapeutic approach in which autologous hematopoietic stem and progenitor (HSPC) cells or T cells are gene edited ex vivo and reinfused. Here, we describe a CRISPR-based gene correction permitting regulated expression of FOXP3 protein. We demonstrate that gene editing preserves HSPC differentiation potential, and that edited regulatory and effector T cells maintain their in vitro phenotype and function. Additionally, we show that this strategy is suitable for IPEX patient cells with diverse mutations. These results demonstrate the feasibility of gene correction, which will be instrumental for the development of therapeutic approaches for other genetic autoimmune diseases.

INTRODUCTION

Primary immunodeficiencies comprise a group of genetic immune diseases, which typically present with recurrent infections, but may instead manifest with predominant autoimmunity (*1*, *2*). Over 350 monogenic immune diseases have been described to date, and this number has been rapidly increasing with technological advances in DNA sequencing and expanding accessibility of genetic screening (*1*). The prototype of genetic autoimmunity is immune dysregulation polyendocrinopathy enteropathy and X-linked (IPEX) syndrome, which is a severe X-linked disease with early onset (*2*, *3*). The most frequent autoimmune manifestations of IPEX syndrome include type 1 diabetes, eczema, and life-threatening enteropathy (*4*). Other common autoimmune manifestations include cytopenia, autoimmune hepatitis, and thyroiditis. IPEX syndrome is classified as a Tregopathy, a class of diseases that selectively affect the function of regulatory T cells (T_{regs}) and, in the case of IPEX syndrome, $CD4^+CD25^{high}FOXP3^+$ T_{regs} (*5*, *6*). In patients with IPEX, nonfunctional T_{regs} are produced that are unable to prevent the development of autoimmunity or allergy because they lack the ability to suppress the function and proliferation of effector T (T_{eff}) cells (*7*). In recent years, the pathophysiology of IPEX syndrome has been dissected, but few therapeutic advances have been made, and limited treatment options exist (*2*). Currently, patients with IPEX are treated with pharmacological immunosuppression, which has only partial efficacy in the acute phase of the disease and cannot prevent long-term disease progression (*2*, *4*). Furthermore, administration of immunosuppressive drugs carries the risk of severe side effects associated with toxicity and susceptibility to infections. The only curative treatment available for IPEX is allogeneic hematopoietic stem cell transplantation. However, many patients do not find a suitable donor or suffer from transplant-related complications (*4*).

IPEX syndrome is caused by mutations in the forkhead box protein 3 (*FOXP3*) gene, and over 70 unique mutations throughout the *FOXP3* locus have been identified (*4*, *8*). FOXP3 is a master transcription factor required for the function of T_{regs}, which up-regulates T_{reg}-associated markers, such as CD25 and CTLA-4, and represses proinflammatory cytokine production (*9*). While T_{regs} rely on constitutive FOXP3 expression, T_{eff} cells transiently express FOXP3 following T cell receptor (TCR) activation (*7*). This cell type–specific regulation is a result of a complex network of promoter and enhancer elements (*9*, *10*). The high and persistent FOXP3 expression in T_{regs} is due to epigenetic marks established during T cell development, including the T_{reg}-specific demethylated region (TSDR) (*10*). It has previously been shown that T_{eff} cells require transient FOXP3 expression for intrinsic regulation of proliferation, cytokine production, and TCR signaling (*11*, *12*). According to the current understanding of IPEX, impairment of both T_{eff} and T_{reg} function underlies IPEX syndrome pathology (*2*, *9*). In human T_{eff} cells and T_{regs}, *FOXP3* pre-mRNA is alternatively spliced, and the two predominant spliced isoforms are the full-length ($FOXP3^{FL}$) isoform and a shorter version that lacks exon 2 ($FOXP3^{dE2}$) (*13*, *14*). The $FOXP3^{FL}$ and $FOXP3^{dE2}$ isoforms each represent roughly half of the *FOXP3* expressed; however, the proportion is skewed in different cell activation states and in a number of inflammatory diseases (*14*). Causative IPEX mutations in exon 2 have been described, with a subset of patients presenting with milder clinical phenotypes (*15*, *16*). Because

[1]Division of Stem Cell Transplantation and Regenerative Medicine, Department of Pediatrics, Stanford University School of Medicine, Stanford, CA, USA. [2]Institute for Stem Cell Biology and Regenerative Medicine (ISCBRM), Stanford University School of Medicine, Stanford, CA, USA. [3]Division of Regenerative Medicine, Stem Cells and Gene Therapy, San Raffaele Telethon Institute for Gene Therapy, San Raffaele Scientific Institute, Milan, Italy. [4]APC Microbiome Ireland, University College Cork, Cork, Ireland. [5]Department of Bioengineering, George R. Brown School of Engineering, Rice University, Houston, TX, USA. [6]Phoenix Children's Hospital, Phoenix, AZ, USA. [7]Division of Immunology, Allergy, and Rheumatology, Department of Pediatrics, University of California, Los Angeles, Los Angeles, CA, USA. [8]The Institute for Advanced Materials and Nanotechnology, The Mina and Everard Goodman Faculty of Life Sciences, Ramat-Gan 52900, Israel.
*These authors contributed equally to this work.
†Corresponding author. Email: rosab@stanford.edu

Downloaded from http://advances.sciencemag.org/ on January 15, 2021

these mutations spare the *FOXP3*^{dE2} isoform, it has been suggested that *FOXP3*^{dE2} can partially compensate for *FOXP3*^{FL} loss but that *FOXP3*^{FL} is required for complete T_{reg} and T_{eff} cell function and prevention of IPEX syndrome (*16*).

Because IPEX syndrome is a monogenic immune disease caused by mutations in *FOXP3*, gene therapy could be a useful approach to treat the disease. We previously developed a *FOXP3* gene delivery protocol for ex vivo generation of genetically engineered T_{regs} that uses lentiviral vector (LV)–mediated delivery of copy of the complementary DNA (cDNA) of the full-length isoform of *FOXP3* (*17*). Because this vector expresses FOXP3 under a constitutive promoter, *EF1α*, it is able to convert IPEX patient conventional CD4$^+$ T cells into potent T_{reg}-like suppressor cells. We are currently optimizing the LV-FOXP3 system for use as a T cell–based therapy for patients with IPEX. However, this approach does not address other cell types, such as T_{eff} cells, that also contribute to the IPEX pathology. An additional limitation of this approach is that it cannot be used on long-term repopulating hematopoietic stem and progenitor cells (HSPCs) because of the adverse effects of FOXP3 overexpression on stem cell proliferation and differentiation (*18*). For the development of a successful *FOXP3* gene therapy using HSPCs, it is necessary to achieve constitutive expression of FOXP3 in the T_{reg} compartment to restore suppressive function without having FOXP3 overexpression perturb the proliferation and function of HSPCs or T_{eff} cells. To maintain this cell type–specific expression, an ideal approach would precisely deliver *FOXP3* to its endogenous gene locus and allow regulation of *FOXP3* in its own genomic context.

To deliver the *FOXP3* cDNA in a site-specific manner while preserving endogenous regulation, we propose gene editing with the clustered regularly interspaced short palindromic repeat (CRISPR)–CRISPR-associated protein 9 (Cas9) system. In general, this one-size-fits-all cDNA insertion approach is designed to benefit all or the majority of patients, given that the causative mutations are located downstream of the insertion site (*19*, *20*). We hypothesized that this site-specific approach would permit gene delivery to patient-derived HSPCs for an autologous transplant. This gene correction approach could provide a more complete and long-term treatment for IPEX syndrome and circumvent the need for matched hematopoietic stem cell donors. Here, we combine the CRISPR system with a DNA repair homology donor to insert the *FOXP3* cDNA into the endogenous locus via homology-directed repair (HDR). We report that this gene editing platform can accurately and specifically target *FOXP3* in HSPCs and that edited HSPCs maintain normal differentiation potential in vitro and in vivo in immunodeficient mice. We demonstrate that both T_{regs} and T_{eff} cells retain their key biologic properties when the cDNA is inserted into the endogenous locus, including normal proliferation of T_{eff} cells. We show that the *FOXP3* gene can be corrected in cells from patients with IPEX with diverse mutations, which demonstrates the feasibility of a CRISPR-based *FOXP3* gene correction approach for IPEX syndrome.

RESULTS

Efficient and precise editing of *FOXP3* locus in human HSPCs and T cells using CRIS

To achieve gene editing at the *FOXP3* locus, we designed a CRISPR system targeting the *FOXP3* gene downstream of the translation start codon in exon 1 (E1) and a corresponding HDR donor containing *FOXP3* cDNA (Fig. 1A). The donor construct was designed to insert a codon-diverged *FOXP3* cDNA and restore wild-type (WT) FOXP3 protein expression in patient cells with diverse and scattered *FOXP3* mutations. The gene replacement donor template was also designed to knock-in a marker gene, the truncated nerve growth factor receptor (*tNGFR*), which is used clinically as a surface marker for selection and tracking of genetically engineered cells. We placed *tNGFR* under the control of a constitutive promoter such that it would be expressed independently of *FOXP3*. Polyadenylation (pA) signals were included in the construct to ensure termination and inactivation of the downstream endogenous gene elements. In addition to the full-length *FOXP3* cDNA construct (*FOXP3*^{FL}), we also developed two similar experimental constructs including a *FOXP3* cDNA of a naturally occurring alternatively spliced isoform of *FOXP3* lacking exon 2 (*FOXP3*^{dE2}) and a *FOXP3* knockout (*FOXP3*^{KO}) construct that disrupts the *FOXP3* gene by inserting only the *tNGFR* maker gene flanked by pA signals (fig. S1A).

We screened *FOXP3* CRISPR single-guide RNAs (sgRNAs) for on-target cutting activity in immortalized K562 cells (Fig. 1B, fig. S1B, and table S1). The sgRNAs 1 and 2 triggered the highest on-target activity (26 ± 7% and 20 ± 5%, respectively, mean ± SD, n = 4) (Fig. 1B), as indicated by the frequency of insertion deletion (indel) mutations detected by TIDE analysis (*21*). Of the sgRNAs screened, sgRNA 2 was selected because of a combination of its on-target activity, safe predicted off-target profile, location in the coding sequence of the gene, and proximity to the start codon. Cutting efficiency of sgRNA 2 was 28 ± 6% in human CD34$^+$ HSPCs and 88 ± 7% in CD4$^+$ T cells (mean ± SD, n = 4), thus validating that the CRISPR system efficiently targets *FOXP3* in the primary cells of interest (Fig. 1, C and D).

Using *FOXP3* sgRNA 2, we edited the allele via the HDR-mediated pathway by transducing HSPCs with a *FOXP3* DNA repair donor delivered as a recombinant adeno-associated virus of serotype 6 (rAAV6) (*22*, *23*). Similarly, we gene edited CD4$^+$ T cells to enable functional testing on T cells. We detected successful HDR as evidenced by an in-out polymerase chain reaction (PCR) amplification of genomic DNA (Fig. 2A and fig. S2A). Precise insertion and the *FOXP3* cDNA sequence were confirmed by sequencing analysis (table S1). Rates of HDR-mediated editing detected by tNGFR expression were 14 ± 7% in primary CD4$^+$CD25^{high} T_{regs} (n = 14), 17 ± 5% in the immortalized MT-2 T_{reg}-like cell line (n = 7) (*24*), 24 ± 10% in CD4$^+$CD25$^{-/low}$ T_{eff} cells (n = 21), and 29 ± 8% in HSPCs (n = 27) (Fig. 2B). Testing of the alternative constructs, *FOXP3*^{dE2} and *FOXP3*^{KO}, in HSPCs revealed average HDR rates of 26 ± 9% and 23 ± 5%, respectively (fig. S2B). To confirm that tNGFR expression was an accurate measure of editing rates, we performed editing on HSPCs from three cell donors and tested editing in each donor in parallel by both tNGFR expression and a quantitative in-out PCR using the Digital Droplet PCR (ddPCR) system (*19*). We found concordance between the two methods of editing detection, 25 ± 2% editing for tNGFR flow cytometry and 29 ± 5% for ddPCR (n = 3), confirming the accuracy of detection (fig. S2C). Mock-treated cells were nucleofected and transduced with rAAV-donor templates in the absence of CRISPR and showed low levels of background episomal tNGFR expression (Fig. 2C and fig. S2D). Enrichment of edited cells using the tNGFR maker resulted in a population consistently above 90% purity (Fig. 2C), confirming that tNGFR could be used to isolate a pure population of edited cells.

Downloaded from http://advances.sciencemag.org/ on January 15, 2021

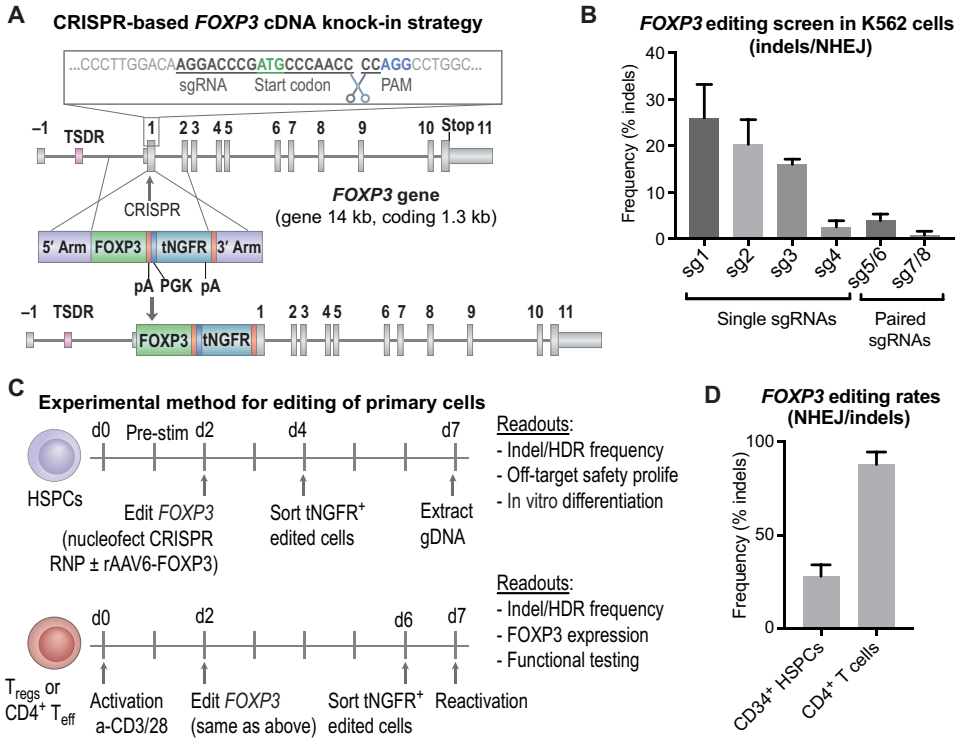


Fig. 1. The *FOXP3* locus is precisely targeted using the CRISPR system in primary HSPCs and T cells. (**A**) Schematic representation of CRISPR-based editing of the *FOXP3* gene showing the CRISPR cut site in first coding exon, E1 (exons depicted by gray boxes separated by lines representing introns; the first coding exon, E1, is preceded by the noncoding exon E-1 and the enhancer with TSDR). A zoomed-in view of the sgRNA binding site relative to the start codon, PAM site, and cleavage site is shown. Homology donor depicted below with arms of homology, codon divergent *FOXP3* cDNA, *BGH* polyadenylation (pA) signal included to terminate the *FOXP3* transcript, truncated NGFR (*tNGFR*) marker gene under the Phosphoglycerate Kinase (*PGK*) promoter to drive marker expression independent of FOXP3 expression, and a second pA. (**B**) Screening of sgRNAs targeting the first coding exon of the *FOXP3* gene. Plasmids encoding WT Cas9 or nickase variant of Cas9 (paired sgRNAs) and *FOXP3* sgRNAs nucleofected into K562 cell lines. CRISPR efficiency measured by TIDE analysis to detect insertion deletion (indel) mutations created by nonhomologous end joining (NHEJ)–mediated DNA repair. (**C**) Experimental method for editing of HSPCs and T cells with functional readouts listed. (**D**) CRISPR cutting efficiency in $CD34^+$ HSPCs and $CD4^+$ T cells quantified by TIDE analysis for the detection of indel mutations created by the NHEJ repair pathway.

Specific FOXP3 gene editing in HSPC using CRISPR

We investigated off-target activity using three complementary methods: bioinformatic prediction, a double-strand break (DSB) capture assay, and next-generation sequencing (NGS). Initially, 58 potential off-target sites were predicted by bioinformatic in silico prediction using the CRISPR Search with Mismatches, Insertions and/or Deletions (COSMID) tool (*25*), of which 96% were in noncoding regions of the genome (fig. S2E and tables S2 and S3, A to E). Ten off-target sites were identified using DSB capture by genome-wide, unbiased identification of DSBs enabled by sequencing (GUIDE)–seq GUIDE-seq (*26*) in the U2OS cell line, of which seven were also predicted by in silico analysis (Fig. 2D and fig. S2F). The 61 sites predicted by the combination of COSMID and GUIDE-seq were then evaluated in *FOXP3* edited HSPCs by NGS. Four sites were validated by NGS, three of which were identified by all three methods. The four sites identified as off-targets were ranked as 1, 3, 4, and 14 by the COSMID algorithm. When excluding a mismatch at the 5′ distal nucleotide, none of the validated sites had more than three mismatches. As compared with the NGS-identified indel rates in the *FOXP3* gene of 42 and 44% in edited cord blood– and bone marrow–derived HSPCs, respectively, all off-target sites had less than 2% targeting (Fig. 2E). None of the validated sites were in coding regions of genes, and on the basis of gene annotation, none of the sites would have a clear impact on hematopoiesis or cell cycle regulation in hematopoietic cells. The results from this off-target analysis suggest that the *FOXP3* CRISPR system is a relatively specific platform for gene editing in hematopoietic cells.

Persistent FOXP3 protein expression and preserved T_{regs} phenotype and function in *FOXP3* edited T_{regs}

We next evaluated our *FOXP3* cDNA insertion strategy in T_{regs}, the major cell type that expresses FOXP3 and is implicated in IPEX syndrome. We used the immortalized MT-2 T_{reg} cell line and primary peripheral blood–derived T_{regs} separated by CD25 enrichment beads. The purity of the primary T_{regs} was confirmed by flow cytometry and epigenetic TSDR demethylation (fig. S3, A and B). We initially tested FOXP3 expression in MT-2 cells and observed that $FOXP3^{FL}$ edited cells expressed FOXP3 protein, but at a lower level compared with unmodified MT-2 cells (Fig. 3A and fig. S4A). In contrast, editing with the $FOXP3^{KO}$ construct led to complete loss of FOXP3 protein expression as predicted (fig. S4B). Insertion of the second isoform of FOXP3 ($FOXP3^{dE2}$) led to approximately 50% FOXP3 expression relative to WT cells (fig. S5A), revealing that delivery of either isoform cDNA individually can support a similar level of FOXP3 expression in T_{regs}. To improve FOXP3 protein expression, we designed two additional constructs: a codon-optimized *FOXP3* cDNA

Downloaded from http://advances.sciencemag.org/ on January 15, 2021

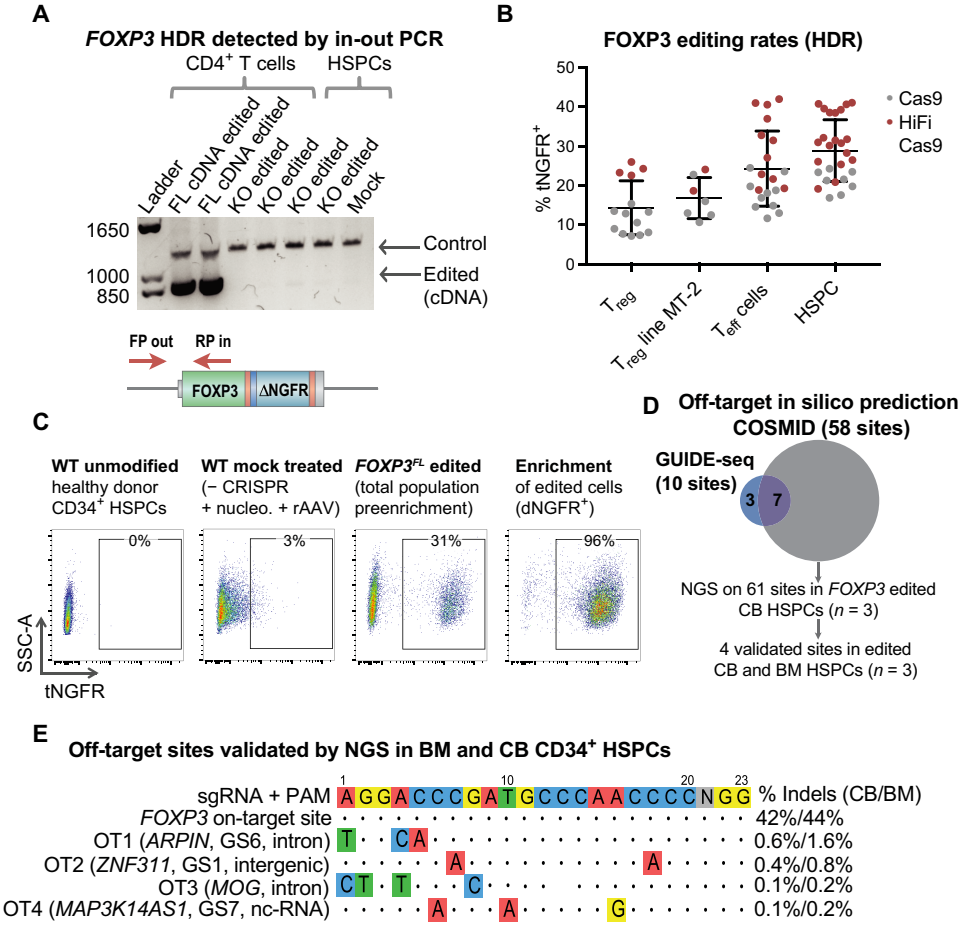


Fig. 2. CRISPR combined with a rAAV6 homology donor enables precise HDR-mediated *FOXP3* cDNA transgene insertion into the endogenous locus. (**A**) Editing observed at the DNA level by an in-out PCR strategy that uses a primer inside the inserted divergent cDNA construct and a second primer outside of the 5′ arm of homology. Control band represents unmodified region in the *FOXP3* gene as a positive control for the presence of genomic DNA. PCR using in-out primers resulted in band only present in samples in which the cDNA was inserted (FL cDNA) and not in *FOXP3* knockout (KO) or mock-treated samples. After the ladder, the first four lanes represent $CD4^+$ T cells, and the last three lanes represent HSPCs. (**B**) Rates of HDR-mediated *FOXP3* editing detected by flow cytometry for tNGFR marker gene expression in primary human $CD4^+CD25^{++}$ T_{regs}, MT-2 T_{reg} cell line, primary $CD4^+CD25^-$ T_{eff} cells, and $CD34^+$ HSPCs. Editing rates with standard Sp Cas9 (gray) and high-fidelity (HiFi) Cas9 (red) are shown for comparison. Dots represent cells from individual donors. (**C**) Representative flow cytometry plots showing tNGFR marker gene expression in edited cord blood–derived $CD34^+$ HSPCs. Negative control: Mock-treated cells nucleofected with phosphate-buffered saline in place of CRISPR and transduced with rAAV6-*FOXP3* donor. Edited cells enriched using tNGFR selection and purity are shown by flow cytometry. SSC-A, side scatter area. (**D**) Venn diagram showing overlap in predicted off-target sites identified by COSMID in silico prediction and GUIDE-seq DSB capture. All predicted sites were tested by NGS in edited $CD34^+$ HSPCs derived from cord blood (CB) and validated by NGS in edited bone marrow (BM)–derived HSPCs. (**E**) The four off-target (OT) sites validated by NGS shown with highlighted mismatches in off-target site versus *FOXP3* sgRNA target sequence, closest gene name, gene region, and average frequency of indel mutations detected by NGS (mean, $n = 3$).

construct ($FOXP3^{FLco}$) and the codon-optimized *FOXP3* construct followed by a woodchuck hepatitis virus posttranscriptional regulatory element ($FOXP3^{co}$ + WPRE or $FOXP3^{FLcoW}$), added to increase mRNA stability and protein translation (Fig. 3B) (*20*). The $FOXP3^{co}$ construct yielded similar FOXP3 protein levels to the $FOXP3^{FL}$ construct, whereas the $FOXP3^{FLcoW}$ construct resulted in moderately increased FOXP3 protein expression levels (Fig. 3C).

We next evaluated FOXP3 expression in human peripheral blood–derived $CD4^+CD25^{high}$ T_{regs}. The pattern of FOXP3 expression from the different donor constructs in MT-2 cells was reflected in peripheral blood–derived T_{regs}. T_{regs} edited with the $FOXP3^{FL}$ cDNA expressed a lower level of FOXP3 protein, and a modest increase in FOXP3 protein expression from the $FOXP3^{FLcoW}$ construct was observed (Fig. 3D). While the various cDNA donors were not able to fully reach WT levels of FOXP3 protein expression in the MT-2 T_{reg} cell line or primary T_{regs}, we hypothesized that this level of FOXP3 protein expression might still be sufficient to restore T_{reg} function.

Immunophenotypic analysis for T_{reg} cell markers, including TIGIT, HELIOS, PD1, CTLA-4, and CD25, revealed that all markers were expressed in *FOXP3* edited T_{regs} (Fig. 3E). The average intensity of HELIOS was decreased after editing, but there was no statistically significant difference in HELIOS expression between edited and mock-treated samples. Overall, the expression levels of all T_{reg} makers were similar in WT and edited T_{regs} with no statistically significant differences observed (Fig. 3E). These results suggest that the CRISPR edited T_{regs} maintain the expression of key proteins characteristic of WT T_{regs}.

Downloaded from http://advances.sciencemag.org/ on January 15, 2021

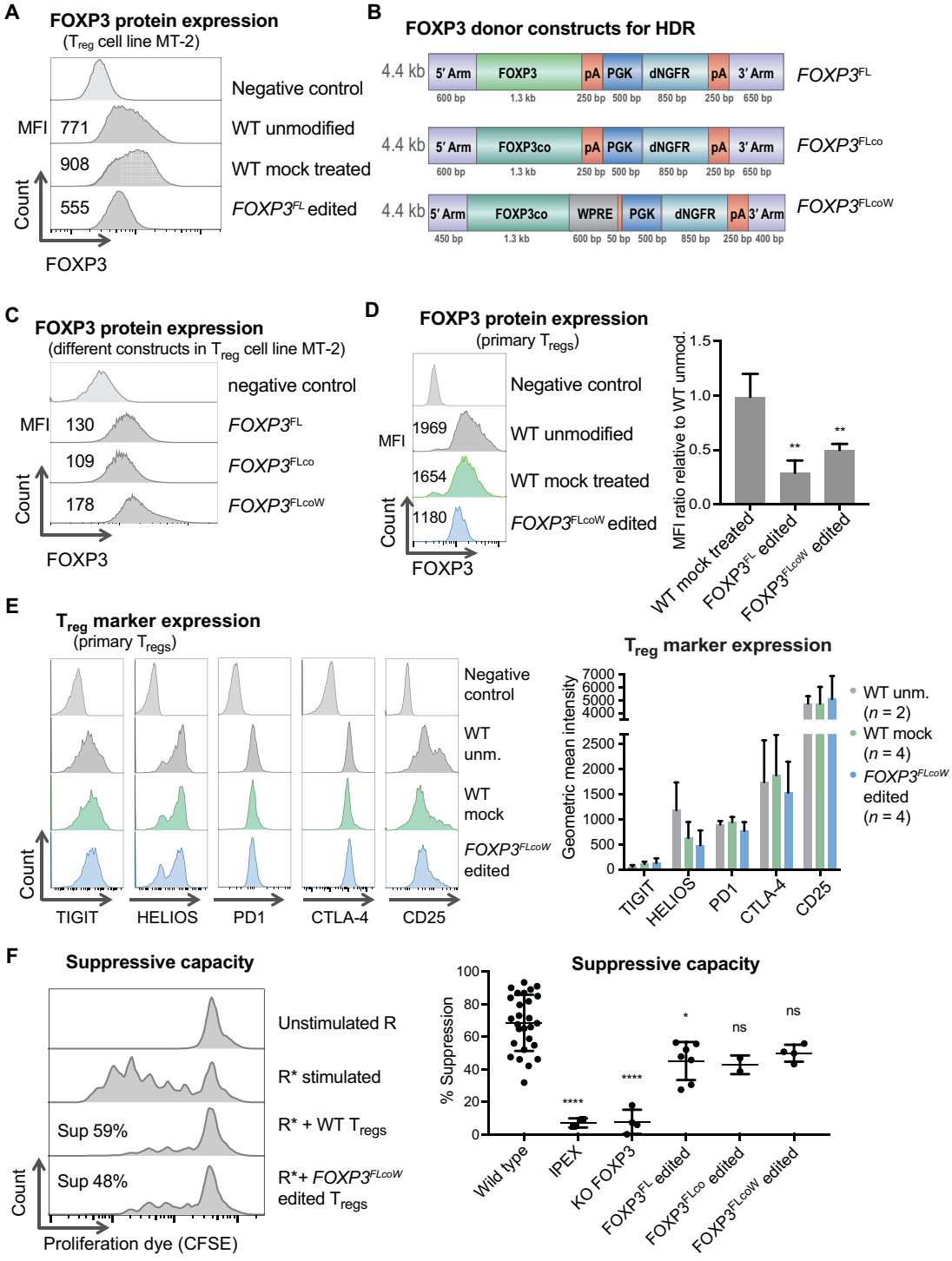


Fig. 3. *FOXP3* edited T_{regs} express FOXP3 protein and display characteristic in vitro phenotype and function. (**A**) Quantification of FOXP3 protein expression in the MT-2 T_{reg} cell line by flow cytometry, showing median fluorescence intensity (MFI) values for one representative experiment out of three performed. (**B**) FOXP3 homology donor constructs designed to improve FOXP3 protein expression, including further codon optimization (*FOXP3*^{FLco}) and addition of a WPRE element (*FOXP3*^{FLcoW}). (**C**) Flow cytometry for FOXP3 in MT-2 cells comparing the different donor constructs. (**D**) FOXP3 expression in primary T_{regs} by flow cytometry and quantification represented as ratio of MFI in treated cells versus WT unmodified T_{regs} [mean ± SD, one-way analysis of variance (ANOVA), Tukey's multiple comparisons]. Significance comparing *FOXP3*^{FL} ($n = 2$, $^{**}P < 0.01$) or *FOXP3*^{FLcoW} ($n = 6$, $^{**}P < 0.01$) to WT mock treated ($n = 2$). (**E**) Expression of signature T_{reg} marker proteins on primary T_{regs} by flow cytometry and corresponding quantification (mean ± SD, $n = 2$ to 4). (**F**) Suppression assay showing unstimulated responders (R), stimulated responders (R*) alone or in coculture with T_{regs}, and calculated percent suppression. Responders stained with proliferation dye, carboxyfluorescein diacetate succinimidyl ester (CFSE). Average suppressive potential over several independent experiments is quantified (right). Significance comparing the WT T_{regs} with following T_{regs}: IPEX, *FOXP3* KO, *FOXP3*^{FL} edited, *FOXP3*^{FLco} edited, and *FOXP3*^{FLcoW} edited (mean ± SD, one-way ANOVA, Tukey's multiple comparisons test, $^{*}P < 0.05$; $^{****}P < 0.0001$; ns, not significant).

Downloaded from http://advances.sciencemag.org/ on January 15, 2021

We next tested the function of gene edited T_{regs} and their hallmark ability to suppress the proliferation of activated T_{eff} cells in a coculture suppression assay. WT T_{regs} from healthy donors displayed suppression capacity at an average of 69 ± 17% (mean ± SD) (Fig. 3F). In contrast, IPEX T_{regs} and *FOXP3* knockout T_{regs} displayed diminished suppression at rates of 7 ± 3% and 8 ± 7%, respectively (Fig. 3F). T_{regs} that were edited with the various *FOXP3* cDNA knock-in constructs all displayed suppressive function, although not fully reaching the level of WT T_{regs} [$FOXP3^{FL}$ 45 ± 12%, $n = 7$, $^*P < 0.05$ versus WT; $FOXP3^{co}$ 43 ± 16%, $n = 2$, P = ns (not significant); $FOXP3^{FLcoW}$ 50 ± 5%, $n = 4$, P = ns] (Fig. 3F). In addition, we tested the suppressive function of $FOXP3^{dE2}$ T_{regs} and found them to perform comparably to $FOXP3^{FL}$ and $FOXP3^{FLcoW}$ edited T_{regs} (fig. S5, B and C). As a negative control, $FOXP3^{FLcoW}$ edited T_{eff} cells that were cultured and edited in parallel were tested and found to lack suppressive function (fig. S5, C and D). Given the ability to suppress T_{eff} proliferation and the relatively higher FOXP3 expression, we selected the $FOXP3^{FLcoW}$ construct for subsequent functional testing. Overall, *FOXP3* cDNA knock-in T_{regs} displayed suppressive function that overlapped with lower normal range of suppressive function observed in WT T_{regs} from different donors, suggesting that editing might be sufficient to restore suppressive capacity to nonfunctional T_{regs}.

Physiologically regulated FOXP3 expression and preserved function in *FOXP3* edited T_{eff} cells

Because T_{eff} cells transiently express FOXP3 upon TCR activation, we monitored FOXP3 protein expression in *FOXP3* edited T_{eff} cells by flow cytometry over a 2-week time course after activation. In nonactivated cells, a low level of background FOXP3 expression was observed, likely due to the pre-editing activation and culturing (Fig. 4A). Upon TCR-mediated reactivation, FOXP3 expression in both edited cells and controls was induced and nearly doubled by day 3 before gradually returning to baseline (Fig. 4A). Overall, the regulation of FOXP3 expression in T_{eff} cells closely mirrored that in WT controls without statistically significant differences, confirming that endogenous regulation of expression was preserved.

In addition to FOXP3 expression, we evaluated the cytokine production profile and proliferation potential of gene edited T_{eff} cells and controls to demonstrate that the intrinsic regulatory effect of FOXP3 was maintained. High levels of interferon-γ (IFN-γ) and low levels of interleukin-2 (IL-2) were produced in both WT and *FOXP3* edited T_{eff} cells (Fig. 4B). IL-17 production was higher in *FOXP3* edited T_{eff} cells, but not statistically different as compared with the WT control (Fig. 4B). In addition, all edited and nonedited T_{eff} cells displayed similar kinetics of activation-induced proliferation over time that was dependent on the strength of activation (Fig. 4C and

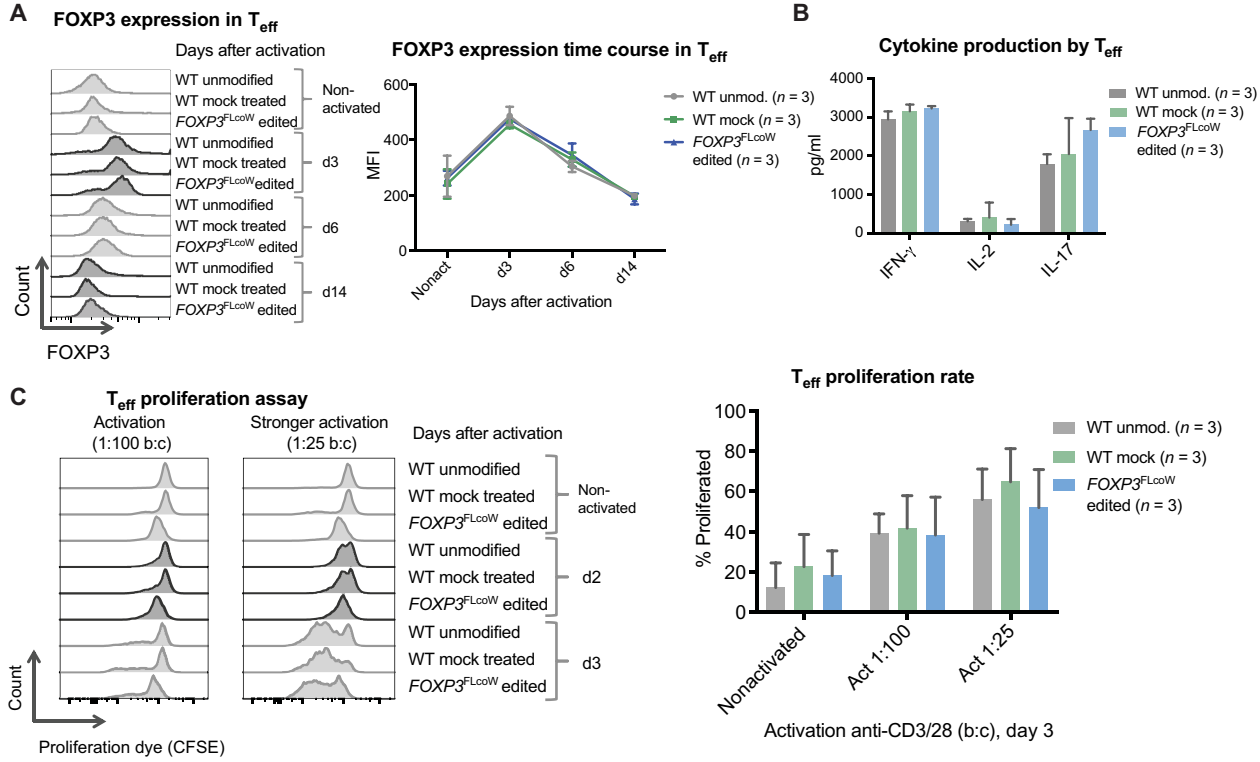


Fig. 4. *FOXP3* editing of T_{eff} cells preserves physiological regulation of FOXP3 expression and in vitro function. (**A**) Flow cytometry time course showing kinetics of FOXP3 expression in nonactivated T_{eff} cells and activated T_{eff} cells on subsequent days after activation [day 3 (d3), d6, and d14], comparing WT unmodified, WT mock-treated, and $FOXP3^{FLcoW}$ edited T_{eff} cells. FOXP3 expression quantified in T_{eff} cells over time course of activation, showing average MFI (mean ± SD, $n = 3$). (**B**) Cytokine production in WT and *FOXP3* gene edited T_{eff} cells determined by enzyme-linked immunosorbent assay (ELISA). Supernatants collected at 24 hours (IL-2) and 48 hours (IFN-γ and IL-17) after activation with anti-CD3/28 (mean ± SD, $n = 3$). (**C**) T_{eff} cell proliferation in response to activation measured by the proliferation assay. Flow cytometry plots of carboxyfluorescein diacetate succinimidyl ester (CFSE) dye–stained T_{eff} cells with progressive dilution of dye as proliferation progresses from nonactivated to day 2 and day 3 after activation with anti-CD3/28 Dynabeads are shown. Comparison of proliferation rates in response to activation with a bead:cell ratio of 1:100 and 1:25. Quantification of average proliferative response of T_{eff} cells from proliferation assay at day 3 is shown to the right, comparing different doses of activation beads (mean ± SD, $n = 3$).

Downloaded from http://advances.sciencemag.org/ on January 15, 2021

fig. S6). Together, these results indicate that *FOXP3* edited T_{eff} cells maintain physiological regulation of FOXP3 expression, cytokine production, and proliferation.

Restored functional FOXP3 expression to IPEX patient T_{regs} and T_{eff} cells after CRISPR-based *FOXP3* editing

We obtained cells from six patients with IPEX, including two sets of brothers with identical pathologic mutations (mutation locations are depicted in Fig. 5A; see table S4 for patient information). Mutations ranged from point mutations to complete abrogation of gene expression. Gene editing of IPEX T cells using the *FOXP3* CRISPR system resulted in precise HDR-mediated editing as revealed by in-out PCR of the edited locus (Fig. 5B). In addition, HDR rates determined by tNGFR expression revealed that IPEX cells could all be targeted with comparable efficiency as healthy donor cells [editing rates for IPEX patients (pt.) 24 and 64 are shown and were reproduced in pt. 37, 65, 77, and 78; Fig. 5C].

Gene editing restored expression of FOXP3 in gene edited IPEX T cells harboring different mutations. We edited IPEX pt. 24 cells, which harbor a c.210+1G>C mutation that disrupts the exon-intron border of the first coding exon and leads to aberrant E1 skipping (*27*). *FOXP3* mRNA isoforms in this patient are shorter due to the missing E1 as shown by reverse transcription (RT)–PCR (Fig. 5D). Gene editing of *FOXP3* in IPEX pt. 24 cells with the full-length *FOXP3* cDNA construct restored expression of the full-length *FOXP3* mRNA isoform (Fig. 5D). We also analyzed mRNA expression after gene editing of T cells from IPEX pt. 37, carrying a c.1150G>A mutation that leads to an alanine-to-threonine amino acid change. RT-PCR and Sanger sequencing revealed that the edited pt. 37 cells expressed *FOXP3* mRNA from the inserted *FOXP3* codon-diverged cDNA construct, as confirmed by a restoration of a codon encoding for the correct alanine residue (Fig. 5E). In addition, the entire mRNA was sequenced to ensure that precise HDR-mediated *FOXP3* cDNA insertion led to the predicted full-length mRNA encoding WT FOXP3 protein. Together, these results provide evidence that the *FOXP3* CRISPR system can be used to restore expression of *FOXP3* in T cells from patients with IPEX with diverse mutations.

We next evaluated proliferative responses of *FOXP3* gene–edited T_{eff} cells from IPEX pt. 77 and 78. Compared with WT healthy donor T_{eff} cells, the T_{eff} cells from both pt. 77 and 78 proliferated at an accelerated rate (Fig. 5F), consistent with previous findings that FOXP3 loss leads to hyperproliferation (*12*). *FOXP3* gene editing was able to normalize proliferation rates closer to the level of healthy donor T_{eff} cells, showing that restoration of FOXP3 expression reestablished regulation of proliferation in IPEX T_{eff} cells (Fig. 5F). To test for restoration of T_{reg}-suppressive activity in IPEX cells, we gene edited T_{regs} of IPEX pt. 64. The WT T_{regs} from healthy donor displayed suppressive function (40%) in coculture conditions with T_{eff} responder cells, whereas IPEX pt. 64 T_{regs} showed diminished suppressive function (4%) (Fig. 5G). Gene editing of IPEX pt. 64 T_{regs} with the $FOXP3^{FLcoW}$ construct was able to increase suppressive function (32%) near the levels typical of healthy donor–edited cells (Fig. 5G), and these results were confirmed on two independent blood draws. Together, the results from functional analyses of edited IPEX T_{reg} and T_{eff} cells show that *FOXP3* correction using the CRISPR system restores physiological regulation of WT FOXP3 expression and has the potential to provide a functional benefit to IPEX patient cells.

We then evaluated the differentiation potential of *FOXP3* edited HSPCs using in vitro and in vivo approaches to confirm safety and feasibility. We performed in vitro colony-forming unit (CFU) assays to test the short-term differentiation of *FOXP3* edited HSPCs into myeloid and erythroid lineages. As compared with WT controls, the *FOXP3* edited HSPCs differentiated into hematopoietic progenitor colonies at similar rates with no statistically significant differences (Fig. 6A). We then tested the in vivo engraftment and multilineage reconstitution of edited HSPCs in a humanized mouse (hu-mouse) model. $FOXP3^{FLcoW}$ edited and control HSPCs (WT unmodified and WT mock) were injected into the liver of 3- to 4-day-old neonatal immunodeficient mice, and engraftment was monitored over a 14-week time course (Fig. 6B). The NSG-SGM3 strain of mice was selected for engraftment studies because of their expression of several human cytokines and their reported higher proportion of $FOXP3^+$ T_{regs} relative to standard NSG mice (*28*). Before injection, edited HSPCs were phenotyped by flow cytometry for purity (%$CD34^+$) and markers of hematopoietic progenitor subsets (fig. S7A). Gene edited and control HSPCs from three cord blood donors were injected, without prior enrichment for tNGFR, into three corresponding litters of mice. A total of 27 mice were injected, including 10 $FOXP3^{FLcoW}$ edited, 9 WT unmodified, and 8 WT mock conditions. The overall survival of the mice over the course of the study was comparable among conditions (fig. S7B). Human cell engraftment, determined by flow cytometric analysis of $hCD45^+$ expression, steadily increased over time in the peripheral blood of the mice and was found to be comparable among conditions with no statistically significant differences (Fig. 6C).

Multilineage human engraftment was observed in the peripheral blood, bone marrow, and spleen in all experimental mice (Fig. 6, D and E). The $tNGFR^+$ edited cells persisted in vivo (fig. S7, C to E), although three mice were excluded for having less than 5% $tNGFR^+$ cells. Analysis of editing rates comparing the proportion of alleles edited by HDR (cDNA insertion) and nonhomologous end joining (NHEJ) (indels) relative to WT alleles in the bone marrow of the mice revealed similar proportions to that of the edited HSPCs before injection with no apparent abnormal expansion of edited cells (fig. S7E). The hematopoietic lineages were analyzed by flow cytometry, and among the edited conditions, the cells were subgated into $tNGFR^+$ and $tNGFR^-$ fractions for comparison (Fig. 6, D and E). We observed the presence of $CD34^+$ HSPCs, $CD56^+$ natural killer cells, $CD13^+$ myeloid cells, $CD19^+$ B cells, and $CD3^+$ T cells in the bone marrow of $FOXP3^{FLcoW}$ edited ($tNGFR^+$ and $tNFGR^-$ fraction) and control mice (Fig. 6, D and E). T cell subsets were further evaluated in the spleen, with $CD3^+$, $CD4^+$ single-positive, $CD8^+$ single-positive, $CD4^+CD8^+$ double-positive, $CD4^+CD25^+FOXP3^+$ T_{regs}, memory $CD4^+CD45RA^-$, and naïve $CD4^+CD45RA^+$ T cells all present in both $FOXP3^{FLcoW}$ edited ($tNGFR^+$ and $tNFGR^-$ fraction) and control mice (Fig. 6, D and E). Some differences in the frequencies of cell subsets were observed between conditions, such as higher proportion of $CD3^+$ cells and a lower proportion of $CD25^+FOXP3^+$ cells in the $tNGFR^+$ fraction. However, no overt changes to immune reconstitution were observed, and each hematopoietic cell lineage was represented among the different experimental conditions (Fig. 6E).

To test the function of T_{regs} and T_{eff} cells derived from in vivo differentiation of edited HSPCs, we sorted $CD3^+CD4^+$ T cells from hu-mouse spleens and separated them into $CD25^{high}$ (T_{reg}) and $CD25^{low}$ (T_{eff}) fractions. The T_{reg} and T_{eff} fractions from the edited conditions were further sorted into $tNGFR^+$ and $tNGFR^-$ fractions. The purity of $FOXP3^+$ T_{regs} within the $CD25^{high}$-sorted fraction was tested by epigenetic TSDR demethylation analysis and found to be

Downloaded from http://advances.sciencemag.org/ on January 15, 2021

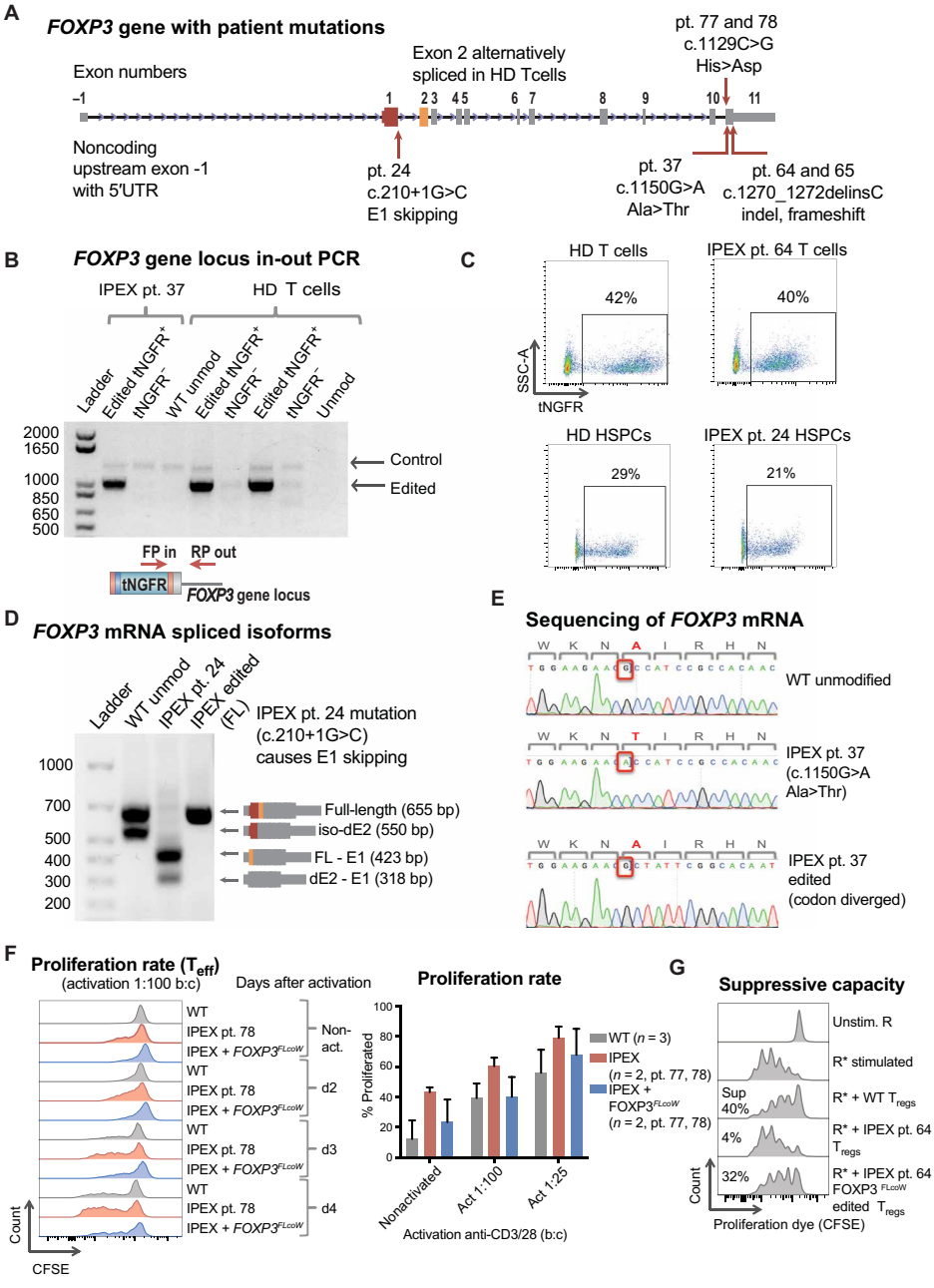


Fig. 5. CRISPR-based editing enables *FOXP3* gene correction in IPEX patient cells. (**A**) Schematic of *FOXP3* gene highlighting mutations of patients involved in this study. (**B**) Editing of IPEX and HD T cells observed at the DNA level by in-out PCR strategy. Forward primer is in the *tNGFR* cassette, and the reverse primer is in the *FOXP3* gene locus outside the 3′ arm of homology. Positive and negative fractions after tNGFR enrichment (+/−) analyzed by PCR. (**C**) Flow cytometry plots of tNGFR staining. (**D**) Expression of *FOXP3* mRNA demonstrated by RT-PCR in activated IPEX and HD T cells (schematic mRNA isoforms are shown to the right of corresponding PCR product bands). After ladder, first lane represents WT cells with two naturally occurring alternatively spliced isoforms, FL and dE2. The second lane shows aberrant skipping of E1 in IPEX pt24 mRNA that results in truncated transcripts. The third lane shows edited IPEX cells with restoration of the FL mRNA. (**E**) Sanger sequencing showing c.1150G>A mutation in the mRNA of pt37, resulting in an Ala>Thr change, and CRISPR-based insertion of divergent *FOXP3* cDNA restoring correct amino acid sequence. (**F**) Proliferation of T_{eff} cells in response to activation measured by the proliferation assay, comparing HD WT cells and IPEX pt78 cells. Quantification of average proliferation response of T_{eff} cells from proliferation assay at day 3. (**G**) Functional testing of gene edited IPEX T_{regs} using the in vitro suppression assay. Flow cytometry plots of CFSE-stained T_{eff} responder cells (R) cultured with or without T_{regs}. Calculated suppressive potential shows diminished suppressive function of IPEX pt. 64 T_{regs}, which was partially restored by *FOXP3* gene editing.

above 78% for the WT unmodified, mock, and *FOXP3*^{FLcoW} edited tNGFR^{-} and undefined for tNGFR^{+} fraction due to low cell count. T_{eff} cells derived from the hu-mouse were found to proliferate at comparable rates to control human peripheral blood–derived T_{eff} cells (fig. S7F). Among hu-mouse–derived T_{eff} cells, all conditions proliferated at similar rates in a dose-dependent manner relative to the strength of activation (fig. S7F). In addition, the CD25^{high}-sorted cells were found to be suppressive upon coculture with responder T_{eff} cells, and the *FOXP3*^{FLcoW} edited T_{regs} displayed comparable suppressive capacity to WT controls (fig. S7G). Overall, these results

Downloaded from http://advances.sciencemag.org/ on January 15, 2021

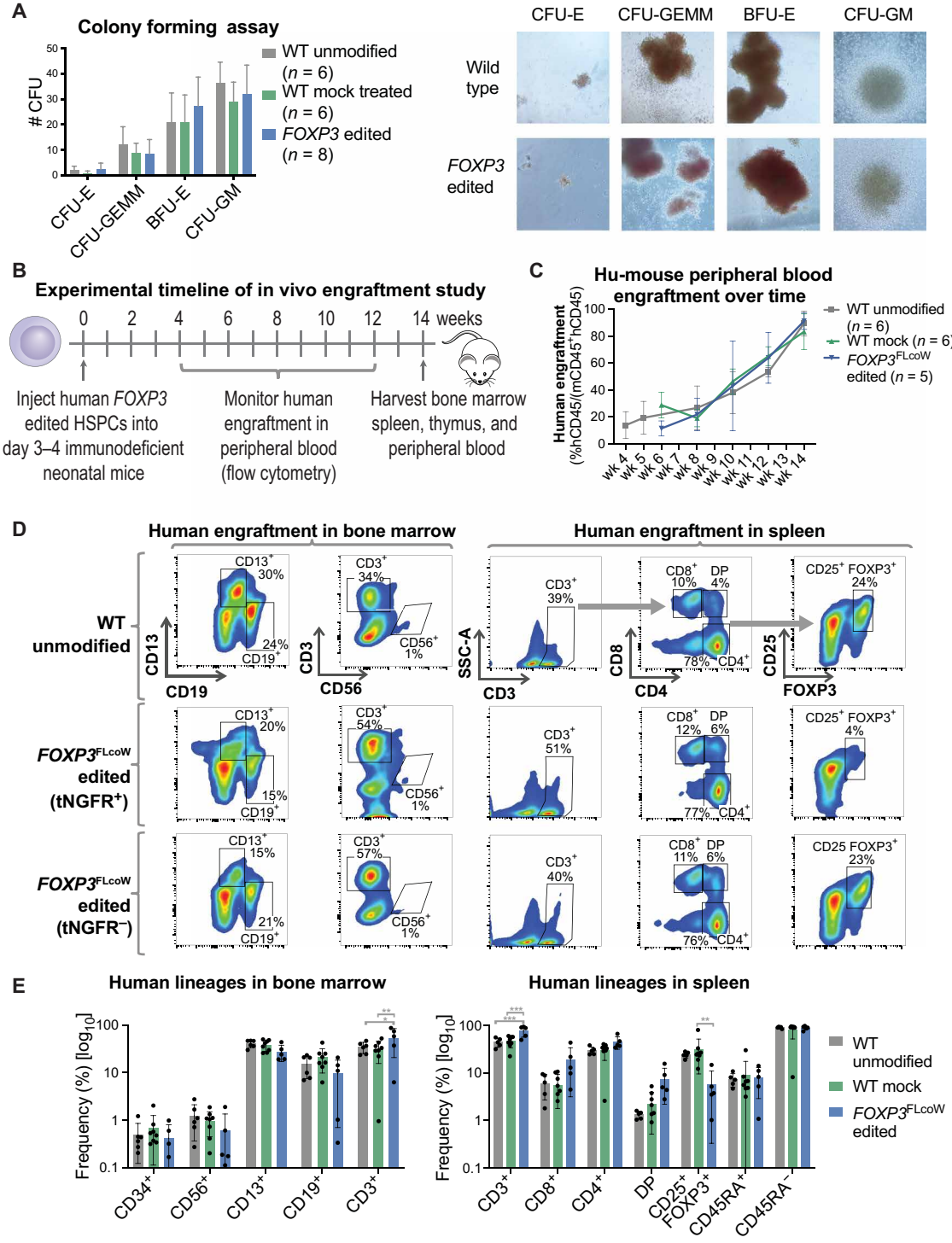


Fig. 6. *FOXP3* edited HSPCs undergo multilineage hematopoietic differentiation and engraftment in vitro and in vivo. (**A**) Differentiation potential of edited HSPCs tested by the in vitro CFU assay. Four resulting hematopoietic progenitor colony types: CFU-E (mature erythroid progenitors), CFU-GEMM (granulocyte, erythrocyte, macrophage, and megakaryocyte), BFU-E (primitive erythroid progenitors), and CFU-GM (granulocyte and macrophage progenitors). Representative images of colonies from the CFU assay, showing similar morphology (×10 magnification). (**B**) Experimental timeline of hu-mouse study using NSG-SGM3 mice. (**C**) Human engraftment kinetics in the peripheral blood of hu-mice at corresponding weeks after injection. Engraftment was measured by flow cytometry for hCD45 marker on human cells, and frequency was quantified relative to the total of human (hCD45$^+$) and mouse (mCD45$^+$) cells (mean ± SD). (**D**) Representative flow cytometry plots of engrafted human hematopoietic subsets in the bone marrow (left) and spleen (right) of hu-mice at 14 weeks after injection. Populations gated out of human cells (hCD45$^+$). *FOXP3* edited samples were divided into tNGFR$^+$ and tNGFR$^-$ gates for comparability. (**E**) Quantification of human hematopoietic lineages by flow cytometry with each symbol representing a single mouse (mean ± SD). In spleen, the CD8$^+$, CD4$^+$, and CD4$^+$CD8$^+$ double-positive (DP) populations were gated out of CD3$^+$ T cells. The CD25$^+$FOXP3$^+$, naïve CD45RA$^+$, and memory CD45RA$^-$ populations were gated out of CD4$^+$ single-positive T cell subset (*P < 0.5, **P < 0.01, ***P < 0.001).

Downloaded from http://advances.sciencemag.org/ on January 15, 2021

demonstrate that *FOXP3* edited HSPCs can engraft in vivo and undergo multilineage differentiation, including the production of functional T_{regs} and T_{eff} cells.

DISCUSSION

Monogenic immune and blood disorders are prime candidates for gene therapy approaches that target autologous HSPCs. Traditionally, viral vectors, such as LVs, that integrate gene cDNAs semirandomly in the genome have been used for gene therapy. While LVs have proven to facilitate efficient gene delivery and are now being widely tested in clinical trials, they are limited in their ability to preserve locus-specific endogenous regulation of gene expression. For this reason, site-specific gene editing has been emerging as a therapeutic approach for the delivery of genes that are regulated by a complex network of noncoding elements. Here, we developed a gene editing approach for IPEX syndrome, which is a prototypical genetic autoimmune disease with unmet medical need. We harnessed site-specific gene editing by the CRISPR system to insert a *FOXP3* cDNA into the endogenous gene locus, preserving spatiotemporal regulation by endogenous regulatory elements.

Using the CRISPR methodology, we efficiently and specifically edited *FOXP3* in HSPCs and in the two main cell types that express FOXP3, T_{regs} and T_{eff} cells. *FOXP3* edited HSPCs did not express FOXP3 protein, whereas edited T_{eff} cells transiently expressed FOXP3 after activation, and edited T_{regs} persistently expressed FOXP3. This cell type–specific expression is consistent with endogenous expression patterns. Edited HSPCs maintained their differentiation potential and displayed a safe off-target profile. Transient FOXP3 expression in T_{eff} cells from healthy donors and patients with IPEX allowed for maintenance of normal proliferative potential and cytokine production capacity. Persistent expression of FOXP3 in T_{regs} preserved their phenotype and ability to suppress T cell function. The level of FOXP3 expression in edited T_{eff} cells closely mirrored that of WT cells, while edited T_{regs} displayed partial FOXP3 protein expression. This cell type–distinct result could be attributed to the fact that T_{regs} physiologically express a much higher level of FOXP3 than activated T_{eff} cells. Although the level of FOXP3 expression in edited T_{regs} led to average suppressive function less than that of WT T_{regs} from normal donors, the suppressive rates of edited cells were still within the lower range of nonedited normal donor function. The range in suppressive function among healthy donor T_{regs} highlights the variability of in vitro regulatory function among individuals. Restoration of a similar level of FOXP3 expression in IPEX patient T_{regs} was sufficient to reestablish suppressive activity in coculture with T_{eff} cell responders.

By using the CRISPR system, we avoided the delivery of *FOXP3* under a constitutive promoter and subsequent FOXP3 overexpression, as in our previously developed LV-EF1α-*FOXP3* vector platform (*17*). The CRISPR gene editing approach prevents the detrimental effects on HSPC proliferation and differentiation caused by *FOXP3* constitutive overexpression (*18*). LV-mediated gene delivery of *FOXP3* with its promoter and enhancer elements has been recently reported in mouse models (*29*). While on the basis of a strong rationale, the capacity to restore spatiotemporally regulated expression of FOXP3 in human IPEX cells using this vector remains to be determined. In general, limitations of LV-mediated delivery include the effect of vector copy number on transgene expression and the potential for position effect variegation. For example, the therapeutic gene could be silenced if positioned into a nonexpressed locus or overexpressed if integrated into a site proximal to a strong promoter or enhancer. In addition, the semirandom insertion of the transgene promoter and enhancer elements into the genome may raise concerns of inadvertently activating proto-oncogenes or genes that would be detrimental to hematopoiesis. These concerns underscore the benefits of site-specific gene editing as a more precise method for therapeutic gene delivery.

In this study, the CRISPR system enabled efficient HDR-mediated editing of *FOXP3* in HSPCs, the cell type used for autologous HSPC transplantation and long-term reconstitution of the immune system. In HSPCs, the overall targeted integration frequency was 29 ± 8% when using tNGFR marker to identify targeted cells. In prior studies, we observed that targeting frequency increased to 50% or greater when the HDR donor was shortened by removal of the *tNGFR* marker gene (*19*). While the tNGFR marker facilitates enrichment of edited cells for functional testing, it may not always be necessary in clinical settings. The marker gene could potentially be removed to improve editing rates if it becomes apparent that selection and tracking of tNGFR-expressing cells are not essential.

While we envision HSPCs being used for autologous transplant, the CRISPR system could be applied to adoptive cell therapy using differentiated T cells or T cell precursor cells. In addition, the efficient CRISPR-based editing of T cells facilitated functional testing of edited T_{regs} and T_{eff} cells. The T cell functional assays performed in this study used the codon-optimized divergent *FOXP3* cDNA sequence followed by a WPRE, which was expected to provide optimal protein expression. To further improve FOXP3 expression and optimize the construct, several avenues may be explored. For example, different codon-diverged sequences could be evaluated in T_{regs}, and modifications to the CG content of the cDNA could be examined. It is also possible that expression from the endogenous *FOXP3* gene and translation of FOXP3 protein are normally enhanced by endogenous intron-exon splice sites and 3′ untranslated region (3′UTR) elements. We did not include endogenous *FOXP3* introns or 3′UTR elements in the cDNA knock-in constructs because of the potential for causing premature crossover events during homologous recombination. Thus, additional future modifications to the construct aimed at improving expression could include incorporation of short exogenous intronic sequences or 3′UTRs from genes highly expressed in T_{regs}.

On the basis of the knowledge that two major spliced isoforms of *FOXP3* are expressed in human T cells, $FOXP3^{FL}$ and $FOXP3^{dE2}$ (*13*, *14*), we speculate that both isoforms could be required to reach WT levels of FOXP3 expression in T_{regs}. We observed that CRISPR-based knock-in of either of the two isoforms leads to partial FOXP3 expression and T_{reg} cell–suppressive function. It has been previously shown that overexpression of either isoform is sufficient to confer T_{reg} function to conventional $CD4^+$ T cells (*13*, *30*, *31*). However, these results could have been confounded by the artificially high level of forced FOXP3 overexpression and the background genomic expression of both isoforms. By comparison, CRISPR-mediated knock-in uses endogenous *FOXP3* promoters and enhancers and allows each isoform to be expressed individually under physiological conditions. Although expression of each isoform was only ~50 to 60% of WT levels, each isoform alone at that level was able to support suppressor function within the lower range of healthy donor cells. Nonetheless, the ability to deliver individual isoforms into the endogenous locus allows the *FOXP3* CRISPR system to be used as a tool to investigate the $FOXP3^{FL}$ and $FOXP3^{dE2}$ isoforms individually.

Downloaded from http://advances.sciencemag.org/ on January 15, 2021

For therapeutic purposes, it may be necessary to use a gene delivery platform that preserves expression of both major *FOXP3* isoforms. In support of this hypothesis, we have previously shown that LV-mediated codelivery of both $FOXP3^{FL}$ and $FOXP3^{dE2}$ cDNAs and subsequent simultaneous overexpression of both isoforms in $CD4^+$ T cells were able to increase FOXP3 protein expression and confer more potent T_{reg} properties than either of the isoforms individually (*13*). Therefore, it is possible that the two isoforms work in concert to regulate a network of T_{reg}-related genes that drive T_{reg} cell function, and the CRISPR system could be used to delineate the distinct and complementary roles of the *FOXP3* isoforms.

The *FOXP3* CRISPR system was similarly used as a tool to study the effects of complete $FOXP3^{KO}$. We observed that *FOXP3* loss in T_{regs} ablated suppressive function. The tNGFR marker was used to isolate a pure population of $FOXP3^{KO}$ cells for functional analysis. The ability to purify *FOXP3*-null cells makes this approach superior to an incomplete knockdown or heterogeneous indel-mediated knockout of *FOXP3* as previously used to investigate the effects of *FOXP3* loss (*11*). Thus, the *FOXP3* CRISPR system allows for the creation of IPEX-like cell models in more readily available healthy donor cells. Similarly, the CRISPR system could be used to knock-in *FOXP3* cDNAs harboring patient-specific mutations, which would provide insight into the molecular mechanisms underlying the heterogeneity of clinical presentation in IPEX syndrome.

While *FOXP3* loss in both $FOXP3^{KO}$ and IPEX T_{regs} abrogated suppressive function, *FOXP3* cDNA knock-in T_{regs} displayed in vitro function and maintained characteristic T_{reg} phenotypic markers. Whether restoring IPEX T_{regs} to the lower range of normal function could be sufficient to provide a stable therapeutic benefit in patients with IPEX remains to be addressed. For example, in the context of certain disease settings such as hemophilia, it has been shown that as little as 5 to 10% gene function can provide therapeutic benefit (*32*–*35*). Moreover, transplanted patients with IPEX with low overall chimerism of donor cells can still undergo tremendous disease regression, especially due to the fact that the T_{reg} compartment shows a selective advantage toward donor cells (*36*–*38*). Similarly, carrier mothers display a selective advantage in the T_{reg} compartment such that the mutated *FOXP3* allele is predominantly located in the inactivated X chromosome, while the WT allele of *FOXP3* is expressed from the active X chromosome in the T_{reg} compartment (*38*). These observations highlight the selective advantage of cells harboring a WT copy of FOXP3 and demonstrate that a small subset of WT T_{regs} can exert a strong protective effect against autoimmunity. We observed that *FOXP3* CRISPR gene editing of IPEX cells led to several improvements, including restoration of WT FOXP3 expression, increased T_{reg}-suppressive function, and normalization of T_{eff} cell proliferation rates.

We evaluated the differentiation potential of *FOXP3* edited HSPCs using a combination of in vitro and in vivo testing. The differentiation of edited HSPCs into myeloid and erythroid lineages was confirmed in vitro. The in vivo studies demonstrated engraftment and multilineage hematopoietic reconstitution and allowed us to observe lymphocyte lineages in more depth. The gene edited cells ($tNGFR^+$ population) persisted in vivo, although in some mice, the percentage of $tNGFR^+$ cells was lower than that in the edited HSPC population before injection. This decrease could be due to several factors, including the previously observed preferential editing of short-term progenitor cells over long-term HSCs and the decrease in cell viability after gene editing (*22*, *39*). However, the lack of expansion of edited cells alleviates any general concerns of clonal expansion of genetically modified cells. This notion is further underscored by the comparable survival rates of hu-mice engrafted with edited and nonedited HSPCs over the course of the study. While there were some differences in cell population frequencies among conditions, there were no major changes or skewing in immune reconstitution. A decrease in the proportion of $FOXP3^+CD25^+$ cells in the $tNGFR^+$ edited condition was found, possibly due to lower FOXP3 protein expression in edited cells. However, edited $FOXP3^+$ T_{regs} isolated from the hu-mouse spleen were found to have similar suppressive capacity to WT counterparts. In addition, hu-mouse–derived *FOXP3* edited T_{eff} cells were found to be functional in vitro and proliferate at comparable rates to WT T_{eff} cells. These functional assays demonstrate that *FOXP3* edited HSPCs retain the capacity to give rise to functional T_{regs} and T_{eff} cells in vivo.

These results lay the foundation for using the *FOXP3* CRISPR system to gene correct autologous HSPCs, T cell precursors, or T_{reg} cells directly for clinical purposes. Ultimately, we envision the CRISPR system being used for *FOXP3* gene repair in IPEX HSPCs for autologous transplantation, circumventing the need to find immunologically matched HSPC donors and lowering the risks associated with transplantation. More broadly, the translation of a CRISPR-based therapy for IPEX syndrome will help pave the way for similar therapeutic approaches in other primary immunodeficiencies with autoimmunity.

MATERIALS AND METHODS

Cell isolation and culture

All research on cells from patients with IPEX and healthy donor controls was approved by the Stanford University Institutional Review Board (IRB) (in accordance with the IRB-approved protocol, IRB-34131) or by the IRB of the Ospedale San Raffaele (protocol TIGET06). Written informed consent was obtained from all patients or patient families. Additional healthy donor HSPCs were isolated from umbilical cord blood donors provided by the Binns Program for Cord Blood Research at the Stanford University or purchased commercially from AllCells or StemCell Technologies. For HSPC isolation from cord blood and bone marrow, mononuclear cells were first obtained by Ficoll-Paque (GE Healthcare) density gradient separation followed by ammonium chloride red blood cell lysis (STEMCELL Technologies). HSPCs were next purified by magnetic cell isolation using the CD34 MicroBead UltraPure Kit (Miltenyi Biotec) according to the manufacturer's recommendations and plated at a cell concentration of 2.5×10^5 cells/ml. The HSPCs were cultured at 37°C with 5% CO_2 and low oxygen (5% O_2) in StemSpan SFEM II medium (STEMCELL Technologies) supplemented with stem cell factor (100 ng/ml; PeproTech), IL-6 (100 ng/ml; PeproTech), thrombopoietin (100 ng/ml; PeproTech), Flt3L (100 ng/ml; PeproTech), 750 nM StemRegenin1 (STEMCELL Technologies), and 35 nM UM171 (STEMCELL Technologies). Additional healthy donor T_{reg} and T_{eff} cells were obtained from the Stanford Blood Center, and peripheral blood mononuclear cells were isolated by Ficoll-Paque density gradient separation. All edited cells were from male donor origin to match male IPEX patient samples, with the exception of a few female mock controls. T_{regs} and T_{eff} cells were separated by magnetic bead isolation using the $CD4^+CD25^+$ Regulatory T Cell Isolation Kit (Miltenyi Biotec) according to the manufacturer's protocol. Both cell fractions were activated with immobilized plate-bound

Downloaded from http://advances.sciencemag.org/ on January 15, 2021

anti-CD3 [10 μg/ml; OKT3 monoclonal antibody (mAb), Miltenyi] with soluble anti-CD28 mAb (1 μg/ml; NA/LE, BD) for 2 to 3 days before editing and then switched to nonactivation conditions. T_{regs} were cultured in X-VIVO 15 (Lonza) with 5% human serum from male AB plasma (Sigma-Aldrich), IL-2 (300 U/ml; PeproTech), and 100 nmol rapamycin (STEMCELL Technologies; only added for certain experiments). T_{eff} cells were cultured in X-VIVO 15, 5% human serum, and IL-2 (50 U/ml). The T_{regs} and T_{eff} cells were cultured at 37°C with 5% CO_2 and ambient oxygen levels. T_{reg}-like MT-2 cells were cultured in X-VIVO 15 with 5% human serum and 1% penicillin/streptomycin. K562 cells (American Type Culture Collection) were cultured in RPMI 1640 medium (Thermo Fisher Scientific) with 10% fetal bovine serum (Thermo Fisher Scientific) at 37°C with 5% CO_2 and ambient oxygen levels. For all cells, fresh medium was added every 2 to 3 days.

Screening of sgRNA efficiency by TIDE analysis

CRISPR chimeric sgRNA was designed using the Desktop Genetics web-based tool (Massachusetts Institute of Technology) and cloned into expression vectors using the px330 plasmid backbone (Addgene). The sgRNAs were placed under the human U6 promoter in the px330 plasmid, which also contained an expression cassette for human codon–optimized SpCas9. For paired sgRNA nickase experiments, the sgRNAs were cloned into the px335 plasmid (Addgene) containing the Cas9 nickase expression cassette and were codelivered as paired plasmids. For the initial screen, 2 μg of sgRNA/Cas9 plasmid DNA was nucleofected into 1 million K562 cells using the Lonza Nucleofector 2b (program T-016). For each reaction, 100 μl of nucleofection solution was used [100 mM KH_2PO_4, 15 mM $NaHCO_3$, 12 mM $MgCl_2.6H_2O$, 8 mM adenosine triphosphate, and 2 mM glucose (pH 7.4)]. The cells were cultured for 2 to 4 days, and genomic DNA was extracted using QuickExtract DNA Extraction Solution (Epicentre) according to the manufacturer's recommendations. The site of DNA cleavage was PCR amplified using Herculase II Fusion Polymerase (Agilent Technologies) and primers flanking the region 5′-CTAGAGCTGGGGTGCAACTATGG-3′ and 5′-GACTACAATACGGCCTCCTCCTCTC-3′. The PCR amplicons were gel purified (Qiagen) and sequenced by Sanger sequencing using the forward primer 5′-CTAGAGCTGGGGTGCAACTATGG-3′. The resulting sequences were used to calculate indel frequencies using the TIDE analysis web-based software (https://tide.nki.nl/). A list of all sgRNA and primer sequences is provided in table S1.

FOXP3 homology donor design

The *FOXP3* cDNA sequence was modified, or diverged, to incorporate synonymous mutations at the nucleotide level according to the redundant codon usage system to prevent premature recombination while still encoding for the WT FOXP3 protein. A constitutive Phosphoglycerate Kinase (*PGK*) promoter was positioned upstream of the *tNGFR* gene such that the marker would be expressed in all edited cells independent of FOXP3 expression. A strong Bovine Growth Hormone (*BGH*) pA signal was positioned after the *FOXP3* cDNA, and another pA was included after the *tNGFR* marker gene to allow independent expression of the *FOXP3* cDNA and tNGFR and to ensure inactivation of the remaining endogenous *FOXP3* locus. The homology arms were centered on the cut site of the sgRNA 2. The 3′ arm (right arm) started at the cut site and reached approximately 650 base pairs (bp) downstream of the cut site, whereas the 5′ arm (left arm) included a region approximately 600 bp upstream of the cut site. The $FOXP3^{FLcoW}$ construct contained a shorter synthetic pA site in place of the *BGH* pA and shorter arms of homology to accommodate the addition of a WPRE element while maintaining an overall similar donor length.

Production of rAAV-*FOXP3* homology donors

All *FOXP3* homology donors were cloned into pAAV-MCS AAV vectors (Agilent Technologies) containing AAV inverted terminal repeats. Cloning was performed using Not I restriction digest [New England Biolabs (NEB)] followed by ligation with T4 DNA ligase (NEB). Plasmid preparation was performed by transforming plasmids into Stbl3 *Escherichia coli* (Life Technologies) and extracting plasmid DNA with Endotoxin-Free Maxi Prep kits (Qiagen). For rAAV production, pAAV-FOXP3 plasmids were cotransfected with rAAV6 helper plasmid DNA into the 293FT Cell Line (Life Technologies). After 72 hours, rAAV6-FOXP3 viral particles were extracted using the AAVpro kit (Clontech, Takara) according to the manufacturer's instructions. The viral stocks were titered using quantitative PCR (qPCR) with primers and probe annealing to the inverted terminal repeats (ITRs). Briefly, the rAAV genomic DNA was isolated using QIAamp MinElute Virus Spin Kit (Qiagen), qPCR was performed on the Roche LightCycler 480, and viral titer (vector genomes per microliter) was calculated using a standard curve generated from a circular pAAV-MCS-donor plasmid of known concentration.

Gene editing by nucleofection and rAAV transduction

Gene editing of primary human HSPCs, T_{regs}, and T_{eff} cells was performed using synthetic sgRNA 2 (5′-AGGACCCGATGCCCAACCCC-3′) complexed to SpCas9 protein [Integrated DNA Technologies (IDT)] as an ribonucleoprotein (RNP) system. The sgRNA was synthesized as a 100-mer RNA molecule with 2′-*O*-methyl 3′phosphorothioate (MS) chemical modifications at the three terminal nucleotides on the 5′ and 3′ ends [5′-2'OMe(A(ps)G(ps)G(ps))ACC CGA UGC CCA ACC CCG UUU UAG AGC UAG AAA UAG CAA GUU AAA AUA AGG CUA GUC CGU UAU CAA CUU GAA AAA GUG GCA CCG AGU CGG UGC UUU 2'OMe(U(ps) U(ps)U)-3′; ps indicates phosphorothioate, and 2'OMe indicates 2′-*O*-methyl]. The sgRNAs were purified by reversed-phase high-performance liquid chromatography (HPLC) and quantified by mass spectrometry. The sgRNAs were purchased from TriLink BioTechnologies and, in later experiments, from Synthego (not HPLC-purified), and editing rates triggered by sgRNAs from the two respective companies were comparable when tested in parallel. The sgRNA was complexed with Cas9 for 10 min at 25°C at an approximate Cas9:sgRNA molar ratio of 1:2.5, using 8 μg of sgRNA and 15 μg of Cas9 per 100 μl of nucleofection solution containing 2.5×10^5 to 1×10^6 cells. After switching to high-fidelity (HiFi) Cas9 (IDT) that showed slightly lower efficiency in parallel experiments, the amount of HiFi Cas9 was increased, and the molar ratio was adjusted to 1:1.8, using 8 μg of sgRNA with 22 μg of HiFi Cas9 per 100 μl of nucleofection solution. The sgRNA/Cas9 complexes were nucleofected into T_{regs} and T_{eff} cells after 2 to 3 days of activation using the P3 Primary Cell Nucleofection Kit (Lonza) and the Lonza Nucleofector 4D (program E-0115). On the day of nucleofection, additional antibiotic (penicillin/streptomycin) was removed from the medium, and rapamycin was removed from the T_{reg} medium. The following day, medium was changed, and antibiotic/rapamycin was replaced. For HSPC editing, the cells were nucleofected using the P3

Downloaded from http://advances.sciencemag.org/ on January 15, 2021

Primary Cell Nucleofection Kit (Lonza) and the Lonza Nucleofector 4D (program DZ-100). For analysis of indel frequencies, genomic DNA was extracted using QuickExtract DNA Extraction Solution (Epicentre), and TIDE analysis was performed as described above. For HDR experiments, rAAV6-FOXP3 donor transduction was performed following nucleofection at a multiplicity of infection (MOI) of 1×10^5 to 1×10^6 viral genomes per cell. After 24 hours of transduction, the medium was changed to remove excess viral particles.

Assessment of HDR-mediated targeted integration by flow cytometry and in-out PCR

To assess HDR at the genomic level, we performed in-out PCR 2 to 4 days after editing using a forward primer outside of the 5′ arm of homology (5′-ATGTCAGCTCGGTCCTTCCA-3′) and a reverse primer inside the inserted divergent cDNA construct (5′-TGGCATAGGATTAAGGGAACTG-3′). A second in-out PCR strategy targeting the 3′ end used a forward primer inside the inserted *tNGFR* region (5′-AGCCTTCAAGAGGTGGAACA-3′) of the construct and a reverse primer in the endogenous *FOXP3* locus outside of the 3′ arm of homology (5′-AGGCCATCCTGATCCTCAC-3′). As a control for the presence of genomic DNA, a PCR strategy targeting a downstream, unmodified region of *FOXP3* was performed (forward primer: 5′-TGCCTCCTCTTCTTCCTTGA-3′; reverse primer: 5′-GAGCCTCGAAAACCCTGACT-3′). Herculase II fusion polymerase (Agilent Technologies) was used for all PCR amplification steps. The resulting PCR products were resolved by agarose gel electrophoresis. For absolute quantification of genomic integration events at the DNA level, an in-out PCR strategy quantified using the ddPCR (Bio-Rad) system was used. For ddPCR, we used two primer/probe sets: the first for the edited region of the *FOXP3* locus (forward primer: 5′-GGGAGGATTGGGAAGACAAT-3′; FAM-labeled probe: 5′-TCAGAGATTGGAGGCTCTCC-3′; reverse primer: 5′-ACAATACGGCCTCCTCCTCT-3′) and a second primer/probe control set targeting a nonmodified region of the *FOXP3* gene used as a reference (forward primer: 5′-CACCGAAATCGGTATTAGTTTG-3′; HEX-labeled probe: 5′-CAGTTCTGGAGGCCAGAGTC-3′; reverse: 5′-CCCGGGGGAGTATAGAAGG-3′). The two regions were amplified and quantified as previously described with modifications (*19*). The PCR used 100 ng of genomic DNA digested with Bam HI-HF (10 U) and an annealing temperature of 62°C. The percentage targeting was calculated as the ratio of FAM (targeted allele) to HEX signal.

Enrichment of tNGFR$^+$ edited cells

Edited tNFGR$^+$ cells were enriched by fluorescence-activated cell sorting (FACS) 2 to 4 days after editing on a FACSAria II SORP (BD Biosciences). Cells were stained with anti-NGFR/CD271 mAb [BioLegend, clone ME20.4, phycoerythrin (PE)–Cy7 conjugated or allophycocyanin (APC) conjugated]. When edited cells were present at low cell numbers, magnetic bead cell isolation was used to increase yield and avoid cell loss associated with FACS. Positive selection of tNGFR$^+$ cells was performed using CD271 (tNGFR) Microbead Kit (Miltenyi Biotec) according to the manufacturer's instructions. Briefly, cells were magnetically labeled with anti-tNGFR microbeads and separated on an MS or LS column in the magnetic field of a MACS separator. Columns were washed and eluted, and the cells were passed through a second column to increase purity.

Off-target analysis

Off-target sites were bioinformatically predicted using the in silico COSMID prediction tool (*25*). For in vitro off-target analysis, GUIDE-seq was performed as previously described (*26*). In brief, the px330-FOXP3-sgRNA2-Cas9 plasmid was electroporated into U2OS cells along with a double-stranded oligodeoxynucleotide (dsODN; 5′-GTTTAATTGAGTTGTCATATGTTAATAACGGTAT-3′). The T7 and restriction fragment length polymorphism (RFLP) assays were performed to confirm editing and tag integration (using TIDE primers 5′-CTAGAGCTGGGGTGCAACTATGG and 5′-GACTACAATACGGCCTCCTCCTCTC-3′). Genomic DNA was extracted, sequencing libraries were prepared, and NGS was performed to identify all sites in which the dsODN was integrated into DNA breaks. GUIDE-seq reads were filtered using a cutoff of eight mismatches according to previous studies on the CRISPR tolerance of mismatches (*25*, *40*). A total of 62 sites identified by the combination of COSMID and GUIDE-seq analyses were then tested by NGS (Illumina MiSeq) in edited HSPCs. HSPCs derived from male healthy donor cord blood ($n = 3$) and bone marrow ($n = 3$) were edited with CRISPR sgRNA2/HiFi Cas9 combined with rAAV6-FOXP3 FL donor, and total cells (tNGFR$^{+/-}$) were used for genomic DNA extraction. NGS reads that were identified at similar rates in edited cells and mock-treated samples were eliminated from the analysis. High background in the mock-treated samples was attributed to the proximity of the sequencing primer to the polynucleotide sequence 5′-CCCC-3′ in the sgRNA target site, as polyN sequences commonly cause errors in NGS and can lead to false-positive indel identification. Only sites with indel mutation rates above mock control background were selected for NGS validation in edited bone marrow–derived HSPCs. Four validated sites were identified in edited bone marrow–derived HSPC, and these sites were analyzed by bioinformatic gene annotation to predict expression in hematopoietic lineages and contribution to hematopoiesis or cell cycle regulation using the UCSC (University of California, Santa Cruz) genome browser, UniProt, GeneCards, and publically archived microarray and RNA sequencing data.

Determination of FOXP3 expression by RT-PCR and flow cytometry

FOXP3 mRNA expression was detected by RT-PCR in *FOXP3*^{FL} edited CD4$^+$ T cells and controls after 3 days of reactivation with Human T-Activator anti-CD3/28 Dynabeads (Life Technologies, 1:25 bead:cell ratio). RNA was extracted with TRI Reagent (Sigma-Aldrich), and polyA$^+$ mRNA was reverse transcribed into cDNA using SuperScript III First-Strand Synthesis System (Thermo Fisher Scientific). PCR amplification of *FOXP3* cDNA was performed using Herculase II fusion polymerase (Agilent Technologies), and primers are listed in table S1. For assessing FOXP3 protein expression by flow cytometry, cells were fixed and permeabilized using FOXP3 staining solutions (eBioscience) and stained with anti-FOXP3 mAb (clone 259D/C7) conjugated to either AF647 (BD Biosciences) or AF488 (BioLegend) following the manufacturer's instructions. Fluorescence was detected on a FACSAria II SORP (BD Biosciences), analyzed using FlowJo software v4 10.5.0, and median florescence intensity (MFI) was recorded.

T_{reg} phenotyping and suppression assay

For T_{reg} phenotyping, cells were stained for flow cytometry using the following antibodies: CD25-BV605 (clone 2A3, BD Biosciences),

Downloaded from http://advances.sciencemag.org/ on January 15, 2021

CTLA-4-PerCPCy5.5 (L3D10, BioLegend), FOXP3-AF647 (259D/C7, BD), HELIOS-PE (22F6, BioLegend), NGFR-BV421 (cME20.4, BioLegend), PD1–fluorescein isothiocyanate (FITC) (MIH4, BD), and TIGIT-PE-Cy7 (MBSA43, eBioscience). Intracellular staining for FOXP3, CTLA-4, and HELIOS was performed after fixing and permeabilizing with FOXP3 staining solutions (eBioscience). Expression was detected on a FACSAria II SORP (BD Biosciences), and geometric mean intensity was analyzed using FlowJo software v4 10.5.0. The function of gene edited T_{regs} was tested by the suppression assay using allogenic $CD4^+$ T cell responders that were labeled with carboxyfluorescein diacetate succinimidyl ester (CFSE) proliferation dye (CellTrace CFSE Cell Proliferation Kit, Life Technologies). Responders were plated at a concentration of 2×10^4 cells per well and cocultured with T_{regs} at a 1:1 or 1:0.5 ratio of responders:suppressors. The cells were activated with a 1:25 ratio of beads:cells using Human T-Activator anti-CD3/28 Dynabeads (Life Technologies). As a reference control, responders were cocultured with an equal number of unstained T_{eff} cells. The cells were cultured in 96-well round well plates and analyzed for CFSE staining on days 3 to 5 using a FACSAria II SORP (BD Biosciences). Nonactivated responders were used for gating, and the percentage of proliferated cells was analyzed using FlowJo software v4 10.5.0. Percent suppression was calculated using the following equation: % suppression = ((%proliferated R^*) – (%proliferated R^* + T_{reg}))/((%proliferated R^*) × 100), where R^* represents stimulated CFSE-stained responder T_{eff}. T_{reg} purity was performed by flow cytometric analysis using the following antibodies: CD4-APC-Cy7 (RPA-T4, BioLegend), CD25-PE (4E3, Miltenyi), CD127-PerCP–Cy5.5 (A019D5, BioLegend), and FOXP3-AF647 (clone 259D/C7, BD). The frequency of demethylated TSDR T_{regs} was quantified by epigenetic bisulfite qPCR in collaboration with Epimune/Epiontis GmbH (Berlin, Germany) as previously described (*41*).

T_{eff} cytokine quantification and proliferation assay

T_{eff} cytokine production was quantified using enzyme-linked immunosorbent assay (ELISA) for IL-2 (BD Biosciences), IFN-γ (BD Biosciences), and IL-17 (R&D Systems). T_{eff} cells were activated using Human T-Activator anti-CD3/28 Dynabeads (Life Technologies) at a 1:25 ratio of beads:cells in 96-well round well plates at 2×10^5 cells per 200 μl. Supernatants were collected at 24 hours (IL-2) and 48 hours (IFN-γ and IL-17) after activation. For the proliferation assay, T_{eff} cells were stained using the CellTrace CFSE Cell Proliferation Kit (Life Technologies) and cultured at 5×10^4 cells per well in 96-well round well plates. The stained cells were activated with a 1:25 ratio of anti-CD3/28 Dynabeads and analyzed for CFSE staining on days 2 to 4 after activation on a FACSAria II SORP (BD Biosciences). The percentage of proliferated cells was determined using FlowJo software v4 10.5.0 and gated using nonactivated responders as a reference.

CFU assay to assess in vitro HSPC differentiation

Gene edited cord blood–derived HSPCs were FACS sorted 2 to 4 days after editing and differentiated in vitro using the CFU assay. For each condition, 500 cells were plated in 1.1 ml of semisolid methylcellulose medium (MethoCult H4434, STEMCELL Technologies) and performed in duplicate or triplicate. The cells suspended in MethoCult were incubated at 37°C with 5% CO_2 and ambient oxygen levels, and the resulting progenitor colonies were counted and scored after 14 days [BFU-E (primitive erythroid progenitors), CFU-E (mature erythroid progenitors), CFU-GM (granulocyte and macrophage progenitors), and CFU-GEMM (granulocyte, erythrocyte, macrophage, and megakaryocyte)].

Engraftment studies in immunodeficient mice

All animal experiments were conducted in accordance with the protocols approved by the Stanford University's Administrative Panel on Laboratory Animal Care Research Committee under the Division of Laboratory Medicine. Human cord blood–derived $CD34^+$ HSPCs were gene edited as described above and injected 2 days after editing (without enriching for $tNGFR^+$ cells). Cultured HSPCs were phenotyped by flow cytometry to ensure purity using the antibodies CD34-PE-Cy7 (4H11, eBioscience), CD38-Percp-Cy5.5 (HIT2, BioLegend), CD45RA-FITC (HI100, BD Biosciences), CD90-APC-Cy7 (5E10, BioLegend), CD49f-PE (GoH3, BioLegend), and combined lineage markers (Lin) on APC as follows: CD45-APC (30-F11, BioLegend), CD19-APC (HIB19, BioLegend), CD14-APC (HCD14, BioLegend), CD235a-APC (HIR2, BioLegend), CD20-APC (2H7, BioLegend), CD16-APC (3G8, BioLegend), CD2-APC (RPA-2.10, BioLegend), CD3-APC (SK7, BioLegend), CD4-APC (SK3, BioLegend), CD8-APC (SK1, BioLegend), and CD13-APC (WM15, BioLegend). On the day of injection, 3- to 4-day-old NSG-SGM3 (the Jackson laboratory, JAX:013062) neonatal pups were irradiated with 100 centigray and rested for 6 hours before injection. HSPCs (between 1.5×10^5 and 1.0×10^6) were resuspended in 30 μl of expansion media, and cells were injected intrahepatically using a 28.5-gauge insulin syringe. Starting at week 6, mice were checked for peripheral engraftment of human $CD45^+$ cells via biweekly retro-orbital bleed. The mice were euthanized between 11 and 14 weeks, and blood, spleen, bone marrow, and thymus were harvested. For blood and spleen samples, red blood cells were lysed following a 5-min incubation on ice with 1× red blood cell lysis buffer (eBioscience) and were resuspended in staining buffer (phosphate-buffered saline, 0.25% bovine serum albumin, and 1 mM EDTA). Cells purified from tissues were stained using the following antibodies: hCD45 BV510 (HI30, BD Biosciences), mCD45-APC (30-F11, BioLegend), CD3-Percp-Cy5.5 (OKT3, BioLegend), CD56-PE (5.1H11, BioLegend), CD13-APC-Cy7 (WM15, BioLegend), and CD19-FITC (HIB19, BD Biosciences). An additional antibody panel for T cell subsets included hCD45 BV510 (HI30, BD Biosciences), mCD45 PE (30-F11, BioLegend), CD4 APC-Cy7 (RPA-T4, BioLegend), CD8 BV650 (SK1, BioLegend), CD25 BV605 (2A3, BD Biosciences), CD45RA FITC (HI100, BD Biosciences), and FOXP3 AF647 (259D, BioLegend). Cells were either analyzed by flow cytometric analysis (CytoFLEX BD) or sorted (BD, FACSAria). Sorted $CD25^{high}$ and $CD25^{low}$ populations were analyzed by suppression and proliferation assays, respectively, as described above.

Statistical analysis

Statistical analysis was performed using GraphPad Prism software v7.0c (GraphPad Inc.). Averages were represented as mean ± SD, and the number of replicates was indicated in respective figures and figure legends. For comparison of two datasets, two-tailed Student's *t* test was performed (α = 5.0%). For paired donor samples, a paired Student's *t* test was performed (α = 5.0%). Differences between multiple groups were identified using one- or two-way analysis of variance (ANOVA) and Tukey's multiple comparisons test (α = 5.0%). Significances were indicated as $*P < 0.05$, $**P < 0.01$, $***P < 0.001$, and $****P < 0.0001$.

Downloaded from http://advances.sciencemag.org/ on January 15, 2021

SUPPLEMENTARY MATERIALS

Supplementary material for this article is available at http://advances.sciencemag.org/cgi/content/full/6/19/eaaz0571/DC1

View/request a protocol for this paper from *Bio-protocol*.

REFERENCES AND NOTES

1. L. D. Notarangelo, Primary immunodeficiencies. *J. Allergy Clin. Immunol.* **125**, S182–S194 (2010).
2. R. Bacchetta, F. Barzaghi, M.-G. Roncarolo, From IPEX syndrome to *FOXP3* mutation: A lesson on immune dysregulation. *Ann. N. Y. Acad. Sci.* **1417**, 5–22 (2018).
3. E. d'Hennezel, M. Ben-Shoshan, H. D. Ochs, T. R. Torgerson, L. J. Russell, C. Lejtenyi, F. J. Noya, N. Jabado, B. Mazer, C. A. Piccirillo, FOXP3 forkhead domain mutation and regulatory T cells in the IPEX syndrome. *N. Engl. J. Med.* **361**, 1710–1713 (2009).
4. F. Barzaghi, L. C. Amaya Hernandez, B. Neven, S. Ricci, Z. Y. Kucuk, J. J. Bleesing, Z. Nademi, M. A. Slatter, E. R. Ulloa, A. Shcherbina, A. Roppelt, A. Worth, J. Silva, A. Aiuti, L. Murguia-Favela, C. Speckmann, M. Carneiro-Sampaio, J. F. Fernandes, S. Baris, A. Ozen, E. Karakoc-Aydiner, A. Kiykim, A. Schulz, S. Steinmann, L. D. Notarangelo, E. Gambineri, P. Lionetti, W. T. Shearer, L. R. Forbes, C. Martinez, D. Moshous, S. Blanche, A. Fisher, F. M. Ruemmele, C. Tissandier, M. Ouachee-Chardin, F. Rieux-Laucat, M. Cavazzana, W. Qasim, B. Lucarelli, M. H. Albert, I. Kobayashi, L. Alonso, C. Diaz de Heredia, H. Kanegane, A. Lawitschka, J. J. Seo, M. Gonzalez-Vicent, M. A. Diaz, R. K. Goyal, M. G. Sauer, A. Yesilipek, M. Kim, Y. Yilmaz-Demirdag, M. Bhatia, J. Khlevner, E. J. Richmond Padilla, S. Martino, D. Montin, O. Neth, A. Molinos-Quintana, J. Valverde-Fernandez, A. Broides, V. Pinsk, A. Ballauf, F. Haerynck, V. Bordon, C. Dhooge, M. L. Garcia-Lloret, R. G. Bredius, K. Kałwak, E. Haddad, M. G. Seidel, G. Duckers, S. Y. Pai, C. C. Dvorak, S. Ehl, F. Locatelli, F. Goldman, A. R. Gennery, M. J. Cowan, M. G. Roncarolo, R. Bacchetta; Primary Immune Deficiency Treatment Consortium (PIDTC) and the Inborn Errors Working Party (IEWP) of the European Society for Blood and Marrow Transplantation (EBMT), Long-term follow-up of IPEX syndrome patients after different therapeutic strategies: An international multicenter retrospective study. *J. Allergy Clin. Immunol.* **141**, 1036–1049.e5 (2018).
5. A. M. Cepika, Y. Sato, J. M. Liu, M. J. Uyeda, R. Bacchetta, M. G. Roncarolo, Tregopathies: Monogenic diseases resulting in regulatory T-cell deficiency. *J. Allergy Clin. Immunol.* **142**, 1679–1695 (2018).
6. S. F. Ziegler, FOXP3: Of mice and men. *Annu. Rev. Immunol.* **24**, 209–226 (2006).
7. R. Bacchetta, L. Passerini, E. Gambineri, M. Dai, S. E. Allan, L. Perroni, F. Dagna-Bricarelli, C. Sartirana, S. Matthes-Martin, A. Lawitschka, C. Azzari, S. F. Ziegler, M. K. Levings, M. G. Roncarolo, Defective regulatory and effector T cell functions in patients with FOXP3 mutations. *J. Clin. Invest.* **116**, 1713–1722 (2006).
8. E. d'Hennezel, K. Bin Dhuban, T. Torgerson, C. A. Piccirillo, The immunogenetics of immune dysregulation, polyendocrinopathy, enteropathy, X linked (IPEX) syndrome. *J. Med. Genet.* **49**, 291–302 (2012).
9. L. Passerini, F. R. Santoni de Sio, M. G. Roncarolo, R. Bacchetta, *Forkhead box P3*: The peacekeeper of the immune system. *Int. Rev. Immunol.* **33**, 129–145 (2014).
10. J. Huehn, J. K. Polansky, A. Hamann, Epigenetic control of FOXP3 expression: The key to a stable regulatory T-cell lineage? *Nat. Rev. Immunol.* **9**, 83–89 (2009).
11. F. R. Santoni de Sio, L. Passerini, S. Restelli, M. M. Valente, A. Pramov, M. E. Maccari, F. Sanvito, M. G. Roncarolo, M. Porteus, R. Bacchetta, Role of human forkhead box P3 in early thymic maturation and peripheral T-cell homeostasis. *J. Allergy Clin. Immunol.* **142**, 1909–1921.e9 (2018).
12. A. N. McMurchy, J. Gillies, M. C. Gizzi, M. Riba, J. M. Garcia-Manteiga, D. Cittaro, D. Lazarevic, S. D. Nunzio, I. S. Piras, A. Bulfone, M. G. Roncarolo, E. Stupka, R. Bacchetta, M. K. Levings, A novel function for FOXP3 in humans: Intrinsic regulation of conventional T cells. *Blood* **121**, 1265–1275 (2013).
13. S. E. Allan, L. Passerini, R. Bacchetta, N. Crellin, M. Dai, P. C. Orban, S. F. Ziegler, M. G. Roncarolo, M. K. Levings, The role of 2 FOXP3 isoforms in the generation of human $CD4^+$ Tregs. *J. Clin. Invest.* **115**, 3276–3284 (2005).
14. R. K. W. Mailer, Alternative splicing of FOXP3—Virtue and vice. *Front. Immunol.* **9**, 530 (2018).
15. E. Gambineri, S. C. Mannurita, D. Hagin, M. Vignoli, S. Anover-Sombke, S. De Boer, G. R. S. Segundo, E. J. Allenspach, C. Favre, H. D. Ochs, T. R. Torgerson, Clinical, immunological, and molecular heterogeneity of 173 patients with the phenotype of immune dysregulation, polyendocrinopathy, enteropathy, X-linked (IPEX) syndrome. *Front. Immunol.* **9**, 2411 (2018).
16. K. Frith, A. L. Joly, C. S. Ma, S. G. Tangye, Z. Lohse, C. Seitz, C. F. Verge, J. Andersson, P. Gray, The FOXP3Δ2 isoform supports Treg cell development and protects against severe IPEX syndrome. *J. Allergy Clin. Immunol.* **144**, 317–320.e8 (2019).
17. L. Passerini, E. R. Mel, C. Sartirana, G. Fousteri, A. Bondanza, L. Naldini, M. G. Roncarolo, R. Bacchetta, $CD4^+$ T cells from IPEX patients convert into functional and stable regulatory T cells by *FOXP3* gene transfer. *Sci. Transl. Med.* **5**, 215ra174 (2013).
18. F. R. Santoni de Sio, L. Passerini, M. M. Valente, F. Russo, L. Naldini, M. G. Roncarolo, R. Bacchetta, Ectopic FOXP3 expression preserves primitive features of human hematopoietic stem cells while impairing functional T cell differentiation. *Sci. Rep.* **7**, 15820 (2017).
19. M. Pavel-Dinu, C. Lee, G. Bao, E. J. Kildebeck, N. Punjya, C. Sindhu, M. A. Inlay, N. Saxena, S. S. De Ravin, H. Malech, M. G. Roncarolo, K. I. Weinberg, M. H. Porteus, Gene correction for SCID-X1 in long-term hematopoietic stem cells. *Nat. Commun.* **10**, 1634 (2019).
20. N. Hubbard, D. Hagin, K. Sommer, Y. Song, I. Khan, C. Clough, H. D. Ochs, D. J. Rawlings, A. M. Scharenberg, T. R. Torgerson, Targeted gene editing restores regulated CD40L expression and function in X-HIGM T cells. *Blood* **127**, 2513–2522 (2016).
21. E. K. Brinkman, T. Chen, M. Amendola, B. van Steensel, Easy quantitative assessment of genome editing by sequence trace decomposition. *Nucleic Acids Res.* **42**, e168 (2014).
22. R. O. Bak, D. P. Dever, M. H. Porteus, CRISPR/Cas9 genome editing in human hematopoietic stem cells. *Nat. Protoc.* **13**, 358–376 (2018).
23. J. Wang, C. M. Exline, J. J. De Clercq, G. N. Llewellyn, S. B. Hayward, P. W.-L. Li, D. A. Shivak, R. T. Surosky, P. D. Gregory, M. C. Holmes, P. M. Cannon, Homology-driven genome editing in hematopoietic stem and progenitor cells using ZFN mRNA and AAV6 donors. *Nat. Biotechnol.* **33**, 1256–1263 (2015).
24. R. Hamano, X. Wu, Y. Wang, J. J. Oppenheim, X. Chen, Characterization of MT-2 cells as a human regulatory T cell-like cell line. *Cell. Mol. Immunol.* **12**, 780–782 (2015).
25. T. J. Cradick, P. Qiu, C. M. Lee, E. J. Fine, G. Bao, COSMID: A web-based tool for identifying and validating CRISPR/Cas off-target sites. *Mol. Ther. Nucleic Acids* **3**, e214 (2014).
26. S. Q. Tsai, Z. Zheng, N. T. Nguyen, M. Liebers, V. V. Topkar, V. Thapar, N. Wyvekens, C. Khayter, A. J. Iafrate, L. P. Le, M. J. Aryee, J. K. Joung, GUIDE-seq enables genome-wide profiling of off-target cleavage by CRISPR-Cas nucleases. *Nat. Biotechnol.* **33**, 187–197 (2015).
27. L. Passerini, F. Barzaghi, R. Curto, C. Sartirana, G. Barera, F. Tucci, L. Albarello, A. Mariani, P. A. Testoni, E. Bazzigaluppi, E. Bosi, V. Lampasona, O. Neth, D. Zama, M. Hoenig, A. Schulz, M. G. Seidel, I. Rabbone, S. Olek, M. G. Roncarolo, M. P. Cicalese, A. Aiuti, R. Bacchetta, Treatment with rapamycin can restore regulatory T cell function in IPEX patients. *J. Allergy Clin. Immunol.*, S0091-6749(19)32592-8 (2019).
28. E. Billerbeck, W. T. Barry, K. Mu, M. Dorner, C. M. Rice, A. Ploss, Development of human $CD4^+FoxP3^+$ regulatory T cells in human stem cell factor-, granulocyte-macrophage colony-stimulating factor-, and interleukin-3-expressing NOD-SCID IL2Rgamma^{null} humanized mice. *Blood* **117**, 3076–3086 (2011).
29. K. E. Masiuk, J. Laborada, M. G. Roncarolo, R. P. Hollis, D. B. Kohn, Lentiviral gene therapy in HSCs restores lineage-specific Foxp3 expression and suppresses autoimmunity in a mouse model of IPEX syndrome. *Cell Stem Cell* **24**, 309–317.e7 (2018).
30. S. E. Allan, A. N. Alstad, N. Merindol, N. K. Crellin, M. Amendola, R. Bacchetta, L. Naldini, M. G. Roncarolo, H. Soudeyns, M. K. Levings, Generation of potent and stable human $CD4^+$ T regulatory cells by activation-independent expression of FOXP3. *Mol. Ther.* **16**, 194–202 (2008).
31. T. Aarts-Riemens, M. E. Emmelot, L. F. Verdonck, T. Mutis, Forced overexpression of either of the two common human Foxp3 isoforms can induce regulatory T cells from CD4(+) CD25(−) cells. *Eur. J. Immunol.* **38**, 1381–1390 (2008).
32. S. S. De Ravin, X. Wu, S. Moir, L. Kardava, S. Anaya-O'Brien, N. Kwatemaa, P. Littel, N. Theobald, U. Choi, L. Su, M. Marquesen, D. Hilligoss, J. Lee, C. M. Buckner, K. A. Zarember, G. O'Connor, D. M. Vicar, D. Kuhns, R. E. Throm, S. Zhou, L. D. Notarangelo, I. C. Hanson, M. J. Cowan, E. Kang, C. Hadigan, M. Meagher, J. T. Gray, B. P. Sorrentino, H. L. Malech, Lentiviral hematopoietic stem cell gene therapy for X-linked severe combined immunodeficiency. *Sci. Transl. Med.* **8**, 335ra57 (2016).
33. A. C. Nathwani, U. M. Reiss, E. G. Tuddenham, C. Rosales, P. Chowdary, J. McIntosh, M. Della Peruta, E. Lheriteau, N. Patel, D. Raj, A. Riddell, J. Pie, S. Rangarajan, D. Bevan, M. Recht, Y. M. Shen, K. G. Halka, E. Basner-Tschakarjan, F. Mingozzi, K. A. High, J. Allay, M. A. Kay, C. Y. Ng, J. Zhou, M. Cancio, C. L. Morton, J. T. Gray, D. Srivastava, A. W. Nienhuis, A. M. Davidoff, Long-term safety and efficacy of factor IX gene therapy in hemophilia B. *N. Engl. J. Med.* **371**, 1994–2004 (2014).
34. A. C. Nathwani, E. G. Tuddenham, S. Rangarajan, C. Rosales, J. McIntosh, D. C. Linch, P. Chowdary, A. Riddell, A. J. Pie, C. Harrington, J. O'Beirne, K. Smith, J. Pasi, B. Glader, P. Rustagi, C. Y. Ng, M. A. Kay, J. Zhou, Y. Spence, C. L. Morton, J. Allay, J. Coleman, S. Sleep, J. M. Cunningham, D. Srivastava, E. Basner-Tschakarjan, F. Mingozzi, K. A. High, J. T. Gray, U. M. Reiss, A. W. Nienhuis, A. M. Davidoff, Adenovirus-associated virus vector-mediated gene transfer in hemophilia B. *N. Engl. J. Med.* **365**, 2357–2365 (2011).
35. V. Stephan, V. Wahn, F. Le Deist, U. Dirksen, B. Broker, I. Müller-Fleckenstein, G. Horneff, H. Schroten, A. Fischer, G. de Saint Basile, Atypical X-linked severe combined immunodeficiency due to possible spontaneous reversion of the genetic defect in T cells. *N. Engl. J. Med.* **335**, 1563–1567 (1996).
36. M. G. Seidel, G. Fritsch, T. Lion, B. Jürgens, A. Heitger, R. Bacchetta, A. Lawitschka, C. Peters, H. Gadner, S. Matthes-Martin, Selective engraftment of donor $CD4^+25^{high}$ FOXP3-positive T cells in IPEX syndrome after nonmyeloablative hematopoietic stem cell transplantation. *Blood* **113**, 5689–5691 (2009).
37. K. A. Kasow, V. M. Morales-Tirado, D. Wichlan, S. A. Shurtleff, A. Abraham, D. A. Persons, J. M. Riberdy, Therapeutic in vivo selection of thymic-derived natural T regulatory cells

Downloaded from http://advances.sciencemag.org/ on January 15, 2021

following non-myeloablative hematopoietic stem cell transplant for IPEX. *Clin. Immunol.* **141**, 169–176 (2011).
38. S. Di Nunzio, M. Cecconi, L. Passerini, A. N. McMurchy, U. Baron, I. Turbachova, S. Vignola, E. Valencic, A. Tommasini, A. Junker, G. Cazzola, S. Olek, M. K. Levings, L. Perroni, M. G. Roncarolo, R. Bacchetta, Wild-type *FOXP3* is selectively active in $CD4^+CD25^{hi}$ regulatory T cells of healthy female carriers of different *FOXP3* mutations. *Blood* **114**, 4138–4141 (2009).
39. D. P. Dever, R. O. Bak, A. Reinisch, J. Camarena, G. Washington, C. E. Nicolas, M. Pavel-Dinu, N. Saxena, A. B. Wilkens, S. Mantri, N. Uchida, A. Hendel, A. Narla, R. Majeti, K. I. Weinberg, M. H. Porteus, CRISPR/Cas9 β-globin gene targeting in human haematopoietic stem cells. *Nature* **539**, 384–389 (2016).
40. E. M. Anderson, A. Haupt, J. A. Schiel, E. Chou, H. B. Machado, Ž. Strezoska, S. Lenger, S. McClelland, A. Birmingham, A. Vermeulen, A. van Brabant Smith, Systematic analysis of CRISPR–Cas9 mismatch tolerance reveals low levels of off-target activity. *J. Biotechnol.* **211**, 56–65 (2015).
41. U. Baron, J. Werner, K. Schildknecht, J. J. Schulze, A. Mulu, U.-G. Liebert, U. Sack, C. Speckmann, M. Gossen, R. J. Wong, D. K. Stevenson, N. Babel, D. Schürmann, T. Baldinger, R. Bacchetta, A. Grützkau, S. Borte, S. Olek, Epigenetic immune cell counting in human blood samples for immunodiagnostics. *Sci. Transl. Med.* **10**, eaan3508 (2018).

Acknowledgments: We would like to thank all members of the Bacchetta, Roncarolo, and Porteus laboratories for feedback and supportive roles, especially L. Nguyen, BS; A. Cepika, MD, PhD; J. Schulze, PhD; D. Dever, PhD; R. Bak, PhD; and I. Aversa, BS. We appreciate the useful discussions and advice from R. Parkman, MD, and K. Weinberg, MD, and feedback on the manuscript from R. Perriman, PhD. We are grateful for patient participation and the excellent patient care by clinicians and medical staff, including R. Agarwal, MD; K. Weinacht, MD; J. Chu, MD; S. Stone, MSN; S. Loeb, RN, BSN; B. Hines, MD; and S. Wadera, MD. We acknowledge F. Romana Santoni de Sio, PhD, for contribution to experimental protocols. We also thank the Binns Program for Cord Blood Research at the Stanford University, particularly S. Mantri, BS, and L. Ren, BS, who provided umbilical cord blood and HSPC samples. We thank Synthego for help with the chemically modified sgRNAs. We thank patients and their families for their trust in our research. **Funding:** We gratefully acknowledge the support from several grants and awards, including the NIH NIAID (R21 AI123896), the CIRM (DISC2-09526), the Stanford SPARK (1110504-308-DHBTC), and the Sutardja Foundation (1198779-101-GHFBB), and the Cancer Prevention and Research Institute of Texas to G.B. (RR140081 and RR170721), in addition to a donation from an anonymous donor to the Stanford Center for Genetic Immune Diseases (CGID) for immunological studies on the patient samples. M.G. thanks the Stanford University for the tremendous support, including the Stanford Maternal and Child Health Research Institute (MCHRI) Postdoctoral Award (Stanford NIH-NCATS-CTSA, UL1 TR001085) and the Stanford University Office of the Dean Postdoctoral Award (1182084-100-DHDEZ). E.L. received funding support from the Agency for Science, Technology and Research, Singapore and the Stanford Masters of Science in Medicine scholarship.
Author contributions: R.B., M.G., and M.P. designed the study and CRISPR strategy. M.G. and E.L. performed or supervised the experiments, and M.G., E.L., R.B., and M.G.R. interpreted the results and analyzed the data. U.L., S.S., L.F., M.N., A. She., M.P.-D., and A.H. helped with protocol design, performing experiments, and/or data collection. C.M.L. and G.B. performed off-target analysis. M.G. wrote the manuscript, which was edited by R.B., M.P., and M.G.R. Patient samples were provided by the dedicated clinicians, including F.B., L.P., C.S.B., H.K.M., M.G.-L., M.J.B., A.B., and A. Sha. **Competing interests:** M.P. is on the Scientific Advisory Board and has equity in CRISPR Therapeutics and Allogene Therapeutics. The other authors declare that they have no competing interests. **Data and materials availability:** All data needed to evaluate the conclusions in the paper are present in the paper and/or the Supplementary Materials. Additional data related to this paper may be requested from the authors.

Submitted 8 August 2019
Accepted 20 February 2020
Published 6 May 2020
10.1126/sciadv.aaz0571

Citation: M. Goodwin, E. Lee, U. Lakshmanan, S. Shipp, L. Froessl, F. Barzaghi, L. Passerini, M. Narula, A. Sheikali, C. M. Lee, G. Bao, C. S. Bauer, H. K. Miller, M. Garcia-Lloret, M. J. Butte, A. Bertaina, A. Shah, M. Pavel-Dinu, A. Hendel, M. Porteus, M. G. Roncarolo, R. Bacchetta, CRISPR-based gene editing enables *FOXP3* gene repair in IPEX patient cells. *Sci. Adv.* **6**, eaaz0571 (2020).

Downloaded from http://advances.sciencemag.org/ on January 15, 2021

Science Advances

CRISPR-based gene editing enables *FOXP3* gene repair in IPEX patient cells

M. Goodwin, E. Lee, U. Lakshmanan, S. Shipp, L. Froessl, F. Barzaghi, L. Passerini, M. Narula, A. Sheikali, C. M. Lee, G. Bao, C. S. Bauer, H. K. Miller, M. Garcia-Lloret, M. J. Butte, A. Bertaina, A. Shah, M. Pavel-Dinu, A. Hendel, M. Porteus, M. G. Roncarolo and R. Bacchetta

Sci Adv **6** (19), eaaz0571.
DOI: 10.1126/sciadv.aaz0571

ARTICLE TOOLS http://advances.sciencemag.org/content/6/19/eaaz0571

SUPPLEMENTARY MATERIALS http://advances.sciencemag.org/content/suppl/2020/05/04/6.19.eaaz0571.DC1

REFERENCES This article cites 40 articles, 9 of which you can access for free
http://advances.sciencemag.org/content/6/19/eaaz0571#BIBL

PERMISSIONS http://www.sciencemag.org/help/reprints-and-permissions

Use of this article is subject to the Terms of Service

Science Advances (ISSN 2375-2548) is published by the American Association for the Advancement of Science, 1200 New York Avenue NW, Washington, DC 20005. The title *Science Advances* is a registered trademark of AAAS.

Copyright © 2020 The Authors, some rights reserved; exclusive licensee American Association for the Advancement of Science. No claim to original U.S. Government Works. Distributed under a Creative Commons Attribution NonCommercial License 4.0 (CC BY-NC).

Downloaded from http://advances.sciencemag.org/ on January 15, 2021